Recent trends and developments in Fenton processes for industrial wastewater treatment – A critical review

João Peres Ribeiro[a], Maria Isabel Nunes[a *]

[a]Department of Environment and Planning and CESAM - Centre for Environmental and Marine Studies, University of Aveiro, 3810-193, Aveiro, Portugal

*Corresponding author: isanunes@ua.pt; +351 234370200. Departamento de Ambiente e Ordenamento, Universidade de Aveiro. Campus Universitário de Santiago, 3810-193, Aveiro, Portugal

Abstract

This study reviews the recent developments in the application of Fenton processes in real industrial wastewater treatment, focusing on heterogeneous catalysts and catalyst regeneration/reuse. This article presents the features, inherent advantages or drawbacks, and primary experimental results obtained on established and emerging Fenton processes, highlighting the course of innovations and current scenario in a research field that has recently undergone rapid transition. Therefore, a comprehensive literature survey was conducted to review studies published over the last decade dealing with application of Fenton processes to industrial wastewater treatment. The research in this field is primarily focused on discovering or synthesizing new materials to substitute conventional iron salt Fenton catalysts and/or regenerate and reuse the spent catalyst, in contrast to optimizing the application of existing materials. Hence, the emphasis is on producing reusable materials, transitioning from linear to circular economy. Some of the major challenges identified herein include analyzing or improving heterogeneous catalyst lifetime, determining the predominant pathway of heterogeneous and homogeneous catalysis to pollutant degradation, and defining the best layout to incorporate Fenton processes into full-scale treatment plants, particularly its coupling with biological treatment.

Keywords: Advanced oxidation processes, Industrial wastewater, Fenton processes, Iron, Catalyst

Declaration of interest: NONE

Ethics in publishing: The work described in this article was carried out in accordance with The Code of Ethics of the World Medical Association (Declaration of Helsinki) for experiments

involving humans; EC Directive 86/609/EEC for animal experiments; Uniform Requirements for manuscripts submitted to Biomedical journals.

Nomenclature

)) – Ultrasonic irradiation

AC – Activated carbon

AOP – Advanced oxidation processes

AOX – Adsorbable organic halides

BOD_5 – 5-day biochemical oxygen demand

BDD – Boron doped diamond

COD – Chemical oxygen demand

CPC – Compound parabolic collector

CT – Chitosan gel

DOC – Dissolved organic carbon

EDDS – Ethylenediamine-N, N'-disuccinic acid

EDTA – Ethylenediaminetetraacetic acid

HDPE – High-density polyethylene

HRT – Hydraulic retention time

$h\nu$ - UV irradiation

IE – Ion-exchange

MBC – Magnetic biochar composite

MICOS – Mixed-iron coated olive stone

NTA – Nitrilotriacetic acid

PAN – Polyacrylonitrile

PEF – Photo-electro-Fenton

R – organic pollutants

SS – Suspended solids

T – Temperature

t – Treatment time

TOC – Total organic carbon

X – Heterogeneous catalyst surface

ZVAl – Zero valent aluminum

ZVI – Zero valent iron

1. Introduction

It is widely accepted that the toxic and recalcitrant nature of certain industrial wastewater render conventional biological processes ineffective for wastewater treatment. For example, textile (dyeing) wastewater has strong color and high chemical oxygen demand (COD), and certain azo-dyes are either toxic or convertible to carcinogenic and mutagenic compounds under anaerobic conditions (Bae et al., 2015; Guo et al., 2018). Olive-oil mill wastewater contains several grams per liter polyphenols, which are toxic to bacteria used in common biological wastewater treatment plants and increase heavy metal solubility in the aquatic environment (Gernjak et al., 2004; Hodaifa et al., 2013). The cosmetic industry wastewater contains xenobiotics, including numerous toxic chemical compounds, such as phenol derivatives, mixtures of surfactants, dyes, fragrances, and cosolvents. This type of wastewater is also characterized by high levels of suspended solids (SS), fats and oils, detergents, and low BOD_5/COD (biochemical/chemical oxygen demand) that hinder biological treatment (Bautista et al., 2007; Pliego et al., 2012). Pulp bleaching wastewater typically has low biodegradability and high contents of COD, SS, dissolved lignin, color, complexing agents such as EDTA, and several organochlorine compounds, including adsorbable organic halides (AOX), which are of utmost concern due to their toxic effects on fish and zooplankton (Ashrafi et al., 2015; Hubbe et al., 2016; Oller et al., 2011; Toczyłowska-Mamińska, 2017).

In this context, advanced oxidation processes (AOPs) are rapidly emerging technologies with several applications, such as organic pollutant destruction through toxicity reduction, biodegradability improvement, and odor and color removal (Mandal et al., 2010). The AOPs effectively fractionate complex high-molecular weight compounds to simple intermediate compounds, which are part of the bioenergetic cycle of living organisms and therefore compatible with biological treatment. These compounds may include acetic, maleic, and oxalic acids and acetone (Rabelo et al., 2014). Among AOPs, the homogeneous Fenton processes are commonly utilized, as they are based on the Fe-catalyzed decomposition of oxidant H_2O_2 into •OH, which non-selectively destroys organic compounds. The efficiency of such processes may be improved when combined with other techniques, such as UV or sonic irradiation, which yield additional •OH and enhance the regeneration of the Fe^{2+} catalyst from Fe^{3+}. In addition to efficiently removing recalcitrant compounds, Fenton processes have reported the following

advantages: they can be performed at room temperature and atmospheric pressure. The required reagents are readily available and easy to handle; these have shortest reaction time among AOPs. They can be implemented simply, without requiring special equipment, and easily integrated into existing water treatment processes, such as coagulation, filtration, and biological oxidation (Babuponnusami and Muthukumar, 2014; Bokare and Choi, 2014; Hodaifa et al., 2013; Ochando-Pulido et al., 2017).

The primary drawbacks associated with the homogeneous Fenton process are the continuous loss of iron ions and solid sludge formation, which requires further management (Karthikeyan et al., 2011; Kishimoto et al., 2013; Ochando-Pulido et al., 2017; Zhang et al., 2019). Another disadvantage is the high cost of chemicals, particularly H_2O_2 (Babuponnusami and Muthukumar, 2014; Balabanič et al., 2012; Hermosilla et al., 2012). The expenses incurred in the homogeneous Fenton process range from 0.2 to 17.7 €·m^{-3}, which highlights the relevance of the adopted operating conditions and their impact on the overall effectiveness of the method (Cañizares et al., 2009).

To overcome some of these disadvantages, several recent advances have been made regarding the supply of the Fe catalyst in the solid (heterogeneous) state: zero-valent iron has been reported as highly effective in acidic conditions, wherein the surface layer of the catalyst particles oxidizes for in-situ production of Fe^{2+}, through the Fenton process. Synthesis of iron-supporting catalysts has also gained recent attention, with the iron in the synthesized catalyst obtained from either iron minerals or iron salt and generally entrapped or impregnated in a solid support. Iron can also be supplied in its natural mineral state. Oxide hydroxides can be dehydroxylated to their oxide compounds under specific conditions, possibly modifying the size, orientation, dimensionality, and morphology of oxides (Wang et al., 2012). The utilization of waste material is a promising alternative, wherein low-cost residues may be used either as an iron source or as a catalyst support, reducing the exploitation of iron ores and applying circular economy principles. Furthermore, nanomaterials can be suitably applied as Fenton catalysts, because they have a high surface area, low diffusion resistance, are easily accessible to reactants, and have numerous active sites (Wang et al., 2012, 2016). Fig. 1 shows the common Fenton processes, as discussed in this study.

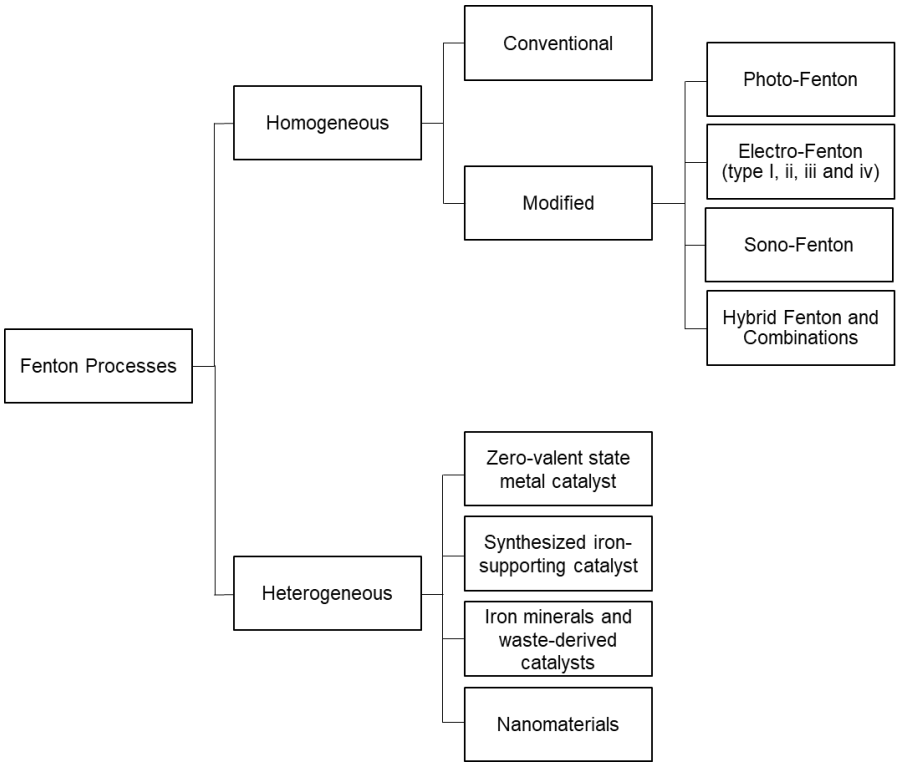

Figure 1. Variations of Fenton processes addressed in the literature and reviewed in this work.

Presently, comprehensive reviews are already available that have focused on applying Fenton processes in wastewater treatment, with various target compounds and process combinations (Ashrafi et al., 2015; Dewil et al., 2017; Kamali and Khodaparast, 2015; Miklos et al., 2018; Wang et al., 2016). However, in the last decade, several improvements have been made to Fenton processes as the research focus transitioned from *process optimization* to actual *process modification*, which was achieved through heterogeneous catalyst development and catalyst recovery or reutilization.

This article aims to critically review the recent trends and developments in the application of Fenton processes to treat real industrial wastewater. It primarily focuses on heterogeneous Fenton catalysis or recovery or reuse of the exhaust catalyst to improve the efficiency of Fenton catalysts, thereby reducing the economic and environmental costs associated with continuous iron consumption and wastage.

2. Methodology

A comprehensive literature survey was conducted using the primary international interdisciplinary platforms for research support in different areas: Science Direct, Scopus, and Web of Science. Combinations of the following keywords were used to conduct the search: “advanced oxidation process”, “Fenton”, “Fenton catalyst”, “heterogeneous catalyst”, and “wastewater”. The “semi-systematic” review approach was followed, according to the classification proposed by Snyder et al. (2019).

As the wastewater characteristics highly influence the effectiveness of Fenton processes, compared to their application in removing synthetic target compounds, this review focuses only on studies dealing with real industrial wastewater. Studies on synthetic wastewaters are only referenced when it is required to discuss the synthesis processes developed recently for novel heterogeneous catalysts.

Herein, literature from the last decade have been considered. A total of 64 articles were reviewed, accounting for 86 case studies, all selected under the conditions stated previously. The subsequent part of this article comprises six sections. Conventional and modified homogeneous Fenton processes are reviewed in Sections 3 and 4, while Sections 5 and 6 aim to present emerging technologies constituting the latest developments reviewed in this study: catalyst regeneration techniques are discussed in Section 5, and Section 6 presents catalyst substitution in the heterogeneous Fenton process. Future challenges in this field of research are discussed in Section 7, and the main conclusions of the study are presented in Section 8. Fig 2 shows the distribution of the reviewed literature by industrial sector, highlighting the increasing attention given to industrial sectors producing wastewaters with large amounts of recalcitrant pollutants, particularly the pulp and paper and textile industries and landfills.

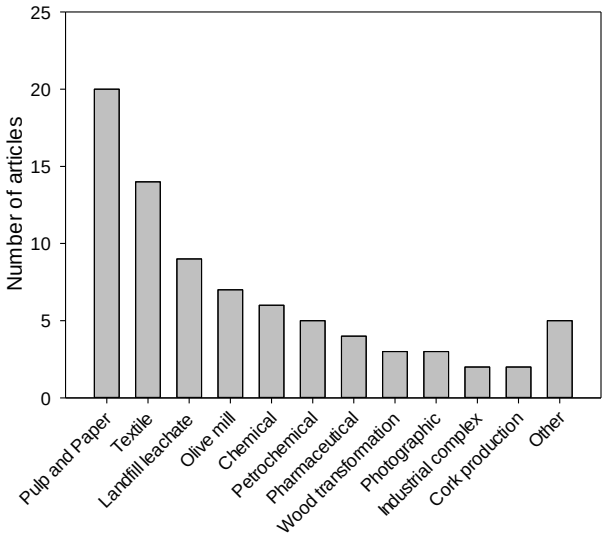

Figure 2. Distribution of the reviewed articles by industrial sector.

3. Conventional homogeneous Fenton process

The overall homogeneous Fenton chemistry is highly complex, including both oxidation and coagulation reactions, and is well described by equations (1)–(14) (Babuponnusami and Muthukumar, 2014; Brink et al., 2017; Hermosilla et al., 2015, 2009; Umar et al., 2010).

$$Fe^{2+} + H_2O_2 \rightarrow Fe(OH)_2^{2+} \rightarrow Fe^{3+} + {}^{\bullet}OH + OH^- \quad k = 40 - 80\ \mathrm{L \cdot mol^{-1} \cdot s^{-1}} \quad (1)$$

$$Fe^{3+} + H_2O_2 \rightarrow Fe^{2+} + {}^{\bullet}O_2H + H^+ \quad k = 10^{-3} - 10^{-2}\ \mathrm{L \cdot mol^{-1} \cdot s^{-1}} \quad (2)$$

$$R + {}^{\bullet}OH \rightarrow R^{\bullet} + H_2O \quad k = 10^{7} - 10^{10}\ \mathrm{L \cdot mol^{-1} \cdot s^{-1}} \quad (3)$$

$$R + {}^{\bullet}OH \rightarrow R{}^{\bullet}OH \quad k = 10^{7} - 10^{10}\ \mathrm{L \cdot mol^{-1} \cdot s^{-1}} \quad (4)$$

$$R^{\bullet} + Fe^{3+} \rightarrow R^+ + Fe^{2+} \quad (5)$$

$$R^+ + OH^- \rightarrow R - OH \quad (6)$$

$$Fe^{2+} + {}^{\bullet}OH \rightarrow Fe^{3+} + OH^- \quad k = (2.5 - 5.0) \times 10^{8}\ \mathrm{L \cdot mol^{-1} \cdot s^{-1}} \quad (7)$$

$$Fe^{2+} + {}^{\bullet}O_2H \rightarrow Fe^{3+} + HO_2^- \quad k = (0.7 - 1.5) \times 10^{6}\ \mathrm{L \cdot mol^{-1} \cdot s^{-1}} \quad (8)$$

$$Fe^{3+} + {}^{\bullet}O_2H \rightarrow Fe^{2+} + O_2 + H^+ \quad k = (0.3 - 2.1) \times 10^{6}\ \mathrm{L \cdot mol^{-1} \cdot s^{-1}} \quad (9)$$

$${}^{\bullet}OH + {}^{\bullet}O_2H \rightarrow H_2O + O_2 \quad k = 1.4 \times 10^{10}\ \mathrm{L \cdot mol^{-1} \cdot s^{-1}} \quad (10)$$

$$2{}^{\bullet}O_2H \rightarrow H_2O_2 + O_2 \quad k = (0.1 - 9.7) \times 10^{7}\ \mathrm{L \cdot mol^{-1} \cdot s^{-1}} \quad (11)$$

$$2{}^{\bullet}OH \rightarrow H_2O_2 \quad k = (5.0 - 8.0) \times 10^{9}\ \mathrm{L \cdot mol^{-1} \cdot s^{-1}} \quad (12)$$

$${}^{\bullet}OH + H_2O_2 \rightarrow {}^{\bullet}O_2H + H_2O \quad k = (1.7 - 4.5) \times 10^{7}\ \mathrm{L \cdot mol^{-1} \cdot s^{-1}} \quad (13)$$

$${}^{\bullet}O_2H + H_2O_2 \rightarrow {}^{\bullet}OH + H_2O + O_2 \quad k = 3.0\ \mathrm{L \cdot mol^{-1} \cdot s^{-1}} \quad (14)$$

Fe^{2+} regeneration (Eq. 2, 5, and 9) is kinetically slow compared to its consumption (Eq. 1), leading a higher Fe^{2+} requirement than commonly needed in catalysts and iron sludge formation (Babuponnusami and Muthukumar, 2014; Garcia-Segura et al., 2016; Umar et al., 2010).

The highly reactive hydroxyl radicals (•OH) produced in the Fenton process control the oxidation of organics (R) in the wastewater by (i) hydrogen abstraction, Eq. (3); (ii) •OH addition, Eq. (4); (iii) radical interaction, Eq. (10)–(12); and (iv) electron transfer, where high-valency ions (or an atom or free radical, if a mono-negative ion is oxidized) are formed, Eq. (1), (7)–(9). High-valence iron intermediates, obtained through visible light absorption by the complex formed between Fe^{3+} and H_2O_2 (ferryl species Fe(IV), denoted as $Fe(OH)_2^{2+}$) also directly react with organic pollutants via the electron transfer pathway (Bautista et al., 2008; Bokare and Choi, 2014; Hermosilla et al., 2015; Sivagami et al., 2018).

Ferric hydroxo-complexes may induce chemical coagulation during the final stage of the Fenton process; chemical coagulation is dominant at lower H_2O_2/Fe^{2+} ratios, while chemical oxidation is dominant at higher ratios (Feng et al., 2010; Umar et al., 2010).

The primary operating conditions affecting the performance of the Fenton processes are pH, oxidant and catalyst concentration, and temperature (Guo et al., 2018; Hermosilla et al., 2015; Mandal et al., 2010). In terms of pH, Fenton processes exhibit maximum catalytic activity at pH approximately 2.5–3.5 (Guo et al., 2018; Hermosilla et al., 2015; Torrades and García-Montaño, 2014). At lower pH values, the iron complex species $[Fe(H_2O)_6]^{2+}$ exist, which reacts more slowly with H_2O_2 than other species (Babuponnusami and Muthukumar, 2014; Guo et al., 2018). Moreover, such high concentrations of H^+ stabilize H_2O_2 to $H_3O_2^+$, inhibiting the regeneration of Fe^{2+} (Bautista et al., 2007; Guo et al., 2018). On the other hand, at higher pH, iron precipitates as $Fe(OH)_3$, which decreases Fe^{2+} in the solution, hinders Fe^{2+} regeneration via Fe^{3+} and H_2O_2 reaction, and favors H_2O_2 decomposition into O_2 and H_2O in basic medium, thus decreasing •OH production.

The degradation rate of organics generally increases with increasing H_2O_2 and Fe^{2+} concentrations, owing to a higher •OH generation (e.g., Rabelo et al., 2014; Ramos et al., 2019; Ribeiro et al., 2020a, 2020b). However, beyond a certain threshold, the increase in concentration decreases organics removal: excess Fe^{2+} results in an increase in the SS content

and electrical conductivity of the treated wastewater, and iron sludge formation; excess H_2O_2 contributes to COD, is harmful to many organisms (e.g., Bautista et al., 2008), and increases scavenging of •OH through competitive reactions indicated by Eq. (7)–(14) (Brink et al., 2017; Guo et al., 2018; He and Zhou, 2017; Ramos et al., 2019; Wang et al., 2016). A method of reducing competitive H_2O_2-consumption reactions involves adding H_2O_2 by stages or as a continuous feed throughout the reaction time. This alleviates the dramatic increase in H_2O_2 concentration and subsequent •OH and $•O_2H$ formation during the initial oxidation stages, avoiding scavenging side reactions and increasing the availability of these species throughout the oxidation process (Munoz et al., 2014; Wang et al., 2016).

Finally, increasing the temperature enhances the kinetics of the process; however, above 50 °C, the decomposition of H_2O_2 towards O_2 and H_2O is favored, whose rate increases by approximately 2.2 times every 10 °C in the range 20–100 °C (Bautista et al., 2008; Lucas and Peres, 2009; Wang et al., 2010). Lal and Garg (2017) reported over 90 % H_2O_2 degradation at 40–60 °C, compared to approximately 70 % degradation at 30 °C.

Table 1 summarizes the experimental studies applying the homogeneous Fenton process for real wastewater treatment. The differences in optimal conditions highlighted the importance of performing optimization studies before application, and the impact of wastewater characteristics on the overall process efficiency. In this manner, advancements in the field of Fenton process application must focus on real wastewater prior to pilot or full-scale implementation.

Table 1. Compilation of results reported on the application of conventional homogeneous Fenton process to real industrial wastewater treatment.

Operating conditions	Wastewater treated	Parameter	Removal (%)	Ref.	Notes
$[H_2O_2]$ = 13.24 mM; $[Fe^{2+}]$ = 3.60 mM; pH = 3.8; t = 60 min; T = 25 ºC	Recycled paper mill wastewater	COD	63.0	Brink et al. (2017)	After 1-day aerobic treatment
		Phenol	> 85.0		
$[H_2O_2]$ = 92.65 mM; $[Fe^{2+}]$ = 3.60 mM; pH = 3.8; t = 60 min; T = 25ºC	Neutral sulphite semi chemical	COD	44.0	Brink et al. (2017)	After 1-day aerobic treatment
		Phenol	> 85.0		
$[H_2O_2]$ = 25 mM; $[Fe^{2+}]$ = 0.90 mM; pH = 2.8; t = 360 min; T = 25ºC	Pulp mill	DOC	48.0	Fernandes et al. (2014)	after anaerobic digestion and yeast treatment
$[H_2O_2]$ = 35 mM; $[Fe^{2+}]$ = 0.90 mM; pH = 2.8; t = 250 min; T = ambient	Pulp mill	DOC	36.0	Lucas et al. (2012)	After biological treatment
$[H_2O_2]$ = 169 mM; $[Fe^{2+}]$ = 12.5 mM; pH = 2.0; t = 10 min; T = 60 ºC	Pulp bleaching wastewater	AOX	82.2	Ribeiro et al. (2020b)	
		COD	8.0		
		BOD_5/COD	0.05 to 0.09		
		Color	2-fold increase		
$[H_2O_2]$ = 29.41 mM; $[Fe^{2+}]$ = 22.38 mM; pH = 7.3; t = 60 min; T = 24 ºC	Pulp bleaching wastewater	COD	62.4	Sevimli et al. (2014)	
$[H_2O_2]$ = 59.2 mM; $[Fe^{2+}]$ = 39.5 mM; pH = 2.8; T = 25 ºC	Reverse osmosis retentate from a recovered paper mill	TOC	50.0 – 60.0	Hermosilla et al. (2012)	
		COD	80.0 – 90.0		
$[H_2O_2]$ = 4.0 mM; $[Fe^{2+}]$ = 4.2 mM; pH = 3.5; t = 30 min; T = ambient	Textile	COD	84.0	Bae et al. (2015)	Preceded by 6 h pure O_2 activated sludge
		Color	77.0		
		Aromatics	78.0		
$[H_2O_2]$ = 48.53 mM; $[Fe^{2+}]$ =3.86 mM; pH = 3.0; t = 120 min; T = ambient	Textile	TOC	64.0	Blanco et al. (2012)	
		COD	70.0		
		Color	96.0		
		SS	99.9		
		Aromatics	96.8		
$[H_2O_2]$ = 44.65 mM; $[Fe^{2+}]$ = 1.19 mM; pH = 3.0; t = 120 min; T = ambient	Textile	TOC	92.0	Blanco et al. (2012)	After 1-day aerobic treatment
		COD	86.0		
		Color	95.6		
		SS	99.9		
		Aromatics	98.0		
$[H_2O_2]$ = 17 mM; $[Fe^{2+}]$ = 1.7 mM; pH = 5.0; t = 35 min; T = 20 ºC	Textile dyeing	TOC	88.2	Feng et al. (2010)	Followed by 18 h membrane bioreactor
		BOD_5/COD	0.10 to 0.44		
		Color	91.3		
$[H_2O_2]$ = 73.5 mM; $[Fe^{2+}]$ = 1.79 mM; pH = 3.0; t = 120 min; T = 25 ºC	Textile	TOC	58.1	Torrades and Montaño (2014)	
		COD	62.9		
$[H_2O_2]$ = 75 mM; $[Fe^{2+}]$ = 50 mM; pH = 2.5; t = 60 min; T = 25 ºC	Landfill leachate	COD	70.0	Hermosilla et al. (2009)	
$[H_2O_2]$ = 800 mM; $[Fe^{2+}]$ = 24.35 mM; pH = 4.0; t = 24 h; T = ambient	Municipal (non-hazardous) landfill leachate	COD	94.0	Trapido et al. (2017)	After 13 day activated sludge treatment, and followed by 1 day activated sludge treatment
		BOD_5	99.0		
		Phenol	100		
$[H_2O_2]$ = 509 mM; $[Fe^{3+}]$ = 6.20 mM; pH = 3.0; t = 240 min; T = ambient	Olive and olive-oil mill (washing step)	COD	97.0	Gassan Hodaifa et al. (2013)	
		Phenol	99.0		
$[H_2O_2]$ = 102.9 mM; $[Fe^{2+}]$ = 6.86 mM; pH = 3.5; t = 60 min; T = 30 ºC	Olive mill	COD	70.0	Lucas and Peres (2009)	
$[H_2O_2]$ = 51.47 mM; $[Fe^{2+}]$ = 26.86 mM; pH = 4.6; t = 90 min; T = ambient	Olive mill	COD	82.4	Ozdemir et al. (2010)	
		Phenol	62.0		
$[H_2O_2]$ = 1000 mM; $[Fe^{2+}]$ = 360 mM; pH = 4.1; t = 60 min; T = ambient	Benzene dye production	TOC	75.2	Guo et al. (2018)	
		COD	85.3		
		BOD_5/COD	0.08 to 0.49		
		Color	99.9		
$[H_2O_2]$ = 26.47 mM; $[Fe^{2+}]$ = 53.72 mM; pH = 3.0; t = 180 min; T = ambient	Chemical industry - production of pyridine	COD	93.9	Padoley et al. (2011)	Followed by 12-day aerobic treatment
$[H_2O_2]$ = 17.65 mM; $[Fe^{2+}]$ = 42.97 mM; pH = 3.0; t = 150 min; T = ambient	Chemical industry - production of 3-cyanopyridine	COD	99.2	Padoley et al. (2011)	Followed by 12-day aerobic treatment
$[H_2O_2]$ = 3268 mM g/L; $[Fe^{2+}]$ = 1.79 mM; pH = 3.0; t = 240 min; T = 120 ºC	Pesticide manufacture	TOC	70.0 - 75.0	Pliego et al. (2012)	After coagulation-adsorption with 0.5 g/L $FeCl_3$ and 4 g/L bentonite
		COD	60.0 - 65.0		

Table 1 (cont.). Compilation of results reported on the application of conventional homogeneous Fenton process to real industrial wastewater treatment.

Operating conditions	Wastewater treated	Parameter	Removal (%)	Ref.	Notes
$[H_2O_2]$ = 2327 mM; $[Fe^{2+}]$ = 1.79 mM; pH = 3.0; t = 240 min; T = 120 ºC	Ink manufacture	TOC	65.0 - 70.0	Pliego et al. (2012)	After coagulation-adsorption with 0.5 g/L $FeCl_3$ and 4 g/L bentonite
		COD	60.0 - 65.0		
$[H_2O_2]$ = 934 mM; $[Fe^{2+}]$ = 1.79 mM; pH = 3.0; t = 240 min; T = 120 ºC	Cosmetic manufacture	TOC	65.0 - 70.0	Pliego et al. (2012)	After coagulation-adsorption with 0.5 g/L $FeCl_3$ and 1 g/L bentonite
		COD	65.0 - 70.0		
$[H_2O_2]$ = 25.03 mM; $[Fe^{2+}]$ = 3.04 mM; pH = 4.0; t = 24 h; T = ambient	Leachate from oil shale processing semicoke landfill area	COD	78.0	Trapido et al. (2017)	After 13 day activated sludge treatment
		BOD_5	96.0		
		Phenol	94.0		
$[H_2O_2]$ = 40 mM; $[Fe^{2+}]$ = 40 mM; pH = 4.0; t = 1.2 h; T = ambient	Coking	COD	75.1	Zhu et al. (2011)	After anaerobic digestion
$[H_2O_2]$ = 1008 mM; $[Fe^{3+}]$ = 122.8 mM; pH = 3.0; t = 30 min; T = 20 ºC	Petroleum refinery	TOC	70.0	Hasan et al. (2012)	
		COD	98.0		
$[H_2O_2]$ = 384 mM; $[Fe^{2+}]$ = 19.05 mM; pH = 3.3; t = 2.2 h; T = ambient	Pharmaceutical	AOX	90.8	Xie et al. (2016)	After anaerobic digestion
		TOC	71.6		
$[H_2O_2]$ = 4.41 mM; $[Fe^{2+}]$ = 0.432 mM; pH = 4.0; t = 60 min; T = 20 ºC	Antibiotic fermentation	COD	96.9	Xing and Sun (2009)	After polyferric sulphate coagulation
		Color	97.3		
		SS	86.7		
$[H_2O_2]$ = 188.2 mM; $[Fe^{3+}]$ = 0.45 mM; pH = 3.0; t = 60 min; T = 120 ºC	Sawmill (from chemical/fungi preservatives wood treatment)	TOC	70.0	Muñoz et al. (2014)	
		COD	80.0		
$[H_2O_2]$ = 402.9 mM; $[Fe^{2+}]$ = 48.9 mM; pH = 4.0; t = 24 h; T = ambient	Plywood industry (from hardwood soaking basin)	COD	99.0	Trapido et al. (2017)	After 3 day activated sludge treatment, and followed by 0.2 day activated sludge treatment
		BOD_5	99.7		
		Phenol	100		
$[H_2O_2]$ = 441.2 mM; $[Fe^{2+}]$ = 11.91 mM; pH = 3.0; t = 50 min; T = ambient	Photographic processing	TOC	80.0	Bensalah et al. (2013)	
$[H_2O_2]$ = 2.765 mM; $[Fe^{2+}]$ = 3.37 mM; pH = 3.0; t = 20 min; T = ambient	Reverse osmosis concentrate from graphical industry	COD	50.0	Van Aken et al. (2013)	
		BOD_5/COD	0.17 to 0.25-0.30		
$[H_2O_2]$ = 1623 mM; $[Fe^{2+}]$ = 65.9 mM; pH = 3.0; t = 60 min; T = 30 – 35 ºC	Industrial complex	COD	80.0	Bianco et al. (2011)	
$[H_2O_2]$ = 3265 mM; $[Fe^{2+}]$ = 21.58 mM; pH = 3.5; t = 30 min; T = 50 ºC	Industrial complex	COD	85.0 – 90.0	Mandal et al. (2010)	
$[H_2O_2]$ = 1306 mM; $[Fe^{2+}]$ = 21.58 mM; pH = 3.5; t = 30 min; T = 50 ºC	Industrial complex	COD	97.0	Mandal et al. (2010)	Followed by Thiobaccilus Ferrooxidans
$[H_2O_2]$ = 1324 mM; $[Fe^{3+}]$ = 4.92 mM; pH = 3.0; t = 160 min; T = ambient	Containers and drum cleaning	TOC	89.6	Gunes et al. (2019)	
		COD	86.8		
		BOD_5	89.1		
		BOD_5/COD	0.42 to 0.38		
$[H_2O_2]$ = 2575 mM; $[Fe^{2+}]$ = 48.4 mM; pH = 3.0; t = 30 min; T= 90 ºC	Wastewater from pipeline cleaning at power plant	TOC	84.0	Pliego et al. (2013)	Iron already present in the wastewater, no external addition needed
		COD	92.0		

4. Modified homogeneous Fenton process

4.1. Photo-Fenton process

In the photo-Fenton process, the degradation of organics is enhanced by UV irradiation via three main pathways: (i) photo-reduction of Fe^{3+} to Fe^{2+}, according to Eq. (15), promoting the regeneration of the catalyst (Zhang et al., 2019); (ii) direct photolysis of H_2O_2 to •OH, according to Eq. (16), which is a slower •OH generation route, usually contributing to a low degradation rate (Xu et al., 2007; Zhang et al., 2019); (iii) photo-decarboxylation of ferric carboxylates,

depending on the ligand-to-metal charge transfer in the complexes formed between Fe^{3+} and the carboxylic acid moiety, as in Eq. (17)–(18) (Garcia-Segura et al., 2016; Hermosilla et al., 2015; Umar et al., 2010).

$$Fe(OH)^{2+} \xrightarrow{h\nu} Fe^{2+} + {}^{\bullet}OH \quad (15)$$

$$H_2O_2 \xrightarrow{h\nu} 2\ {}^{\bullet}OH \quad (16)$$

$$Fe(III)(RCO_2)^{2+} \xrightarrow{h\nu} Fe^{2+} + CO_2 + R^{\bullet} \quad (17)$$

$$R^{\bullet} + O_2 \rightarrow RO_2^{\bullet} \rightarrow \text{products} \quad (18)$$

In addition to the higher degradation rate, the photo-Fenton process decreases the catalytic iron requirement and sludge volume generation (Hermosilla et al., 2015; Ribeiro et al., 2020b, 2020a). Hermosilla et al. (2009) treated landfill leachate using a photo-Fenton process with 32 times less iron and 25 times less sludge volume than the conventional Fenton process, with the same COD removal.

The photo-Fenton process faces certain challenges, such as both process design and process layout complexity, high cost of UV reactors, short operating lifecycle of artificial UV sources, high energy consumption, and the variability and limited availability of solar radiation (Belalcázar-Saldarriaga et al., 2018; Durán et al., 2012; Zhang et al., 2019). Belalcázar-Saldarriaga et al. (2018) removed acid orange 52 dye using the photo-Fenton process at 1 USD·m^{-3}; dealing with real paper mill wastewater, Balabanič et al. (2012) achieved removal at 36.26 €·m^{-3}, and Ribeiro et al. (2020b) at 11 €·m^{-3}, highlighting the significance of selecting real wastewater.

Table 2 presents studies on photo-Fenton treatment of real wastewater, emphasizing the relevance of wastewater characteristics and operating conditions in the treatment results. For instance, Bensalah et al. (2013) achieved 85–90 % total organic carbon (TOC) removal after 50 min from a photographic processing wastewater by, using 88.2 mM H_2O_2 and 3.6 mM Fe^{2+} in a Pyrex photo-reactor and a 40 W low pressure mercury vapor lamp emitting at 254 nm. Eskelinen et al. (2010) reported very low efficiency when dealing with pulp bleaching wastewater for the same H_2O_2 concentration, five times the catalyst concentration (provided as Fe^{3+}), and using a 125 W UV lamp emitting at 254 nm, obtaining only 20 % COD removal after 60 min. This result verifies that the photo-Fenton process using the Fe^{2+} catalyst is highly

efficient, because of the rapid reaction of H_2O_2 with Fe^{2+}, compared to the Fenton-like reaction of H_2O_2 with Fe^{3+}.

Photo-Fenton reactions are driven by low-energy photons (240–400 nm wavelength for the Fe^{2+}/H_2O_2 system and 550 nm for Fe^{3+}/H_2O_2 process), which has increased the investigation of solar-photo-Fenton process over the last few years (Garcia-Segura et al., 2016; Vilar et al., 2009; Zhang et al., 2019). Fernandes et al. (2014) and Lucas et al. (2012) applied solar photo-Fenton to treat Kraft pulp mill wastewater after biological treatment, achieving 90 % dissolved organic carbon (DOC) removal. The former used 41 mM H_2O_2 and 0.18 mM Fe^{2+}, with 19 $kJ \cdot L^{-1}$ solar irradiation; while the latter used 50 mM H_2O_2 and 0.09 mM Fe^{2+}, with 31 $kJ \cdot L^{-1}$ solar irradiation. Both studies were conducted in a pilot-scale solar plant, comprising two compound parabolic collector CPC units (3.02 m^2), with 24 borosilicate tubes connected by flexible HDPE joints, operated in batch mode. These studies reveal a trend of lower iron requirement on applying higher irradiation, because of the increased Fe^{3+} photo-reduction efficiency. The DOC removal using Fenton process was below 40 % in both studies, even with 0.90 mM Fe^{2+}. Furthermore, Vilar et al. (2009) achieved 94 % DOC removal from cork bleaching wastewater using 77.1 mM H_2O_2 and 0.36 mM Fe^{2+}, with 31.5 $kJ \cdot L^{-1}$ solar irradiation. The absence of a biological pre-treatment in this study leads to higher organic competition for •OH, justifying the high chemical consumption and irradiation for similar results as Fernandes et al. (2014) and Lucas et al. (2012).

4.2. Electro-Fenton process

Although the term “electro-Fenton” is generally used to describe the coupling between the Fenton process and electrochemical oxidation, this coupling may be of four different types, depending on the addition or formation mechanism of the Fenton reagent:

(i) Type I is usually referred to as the actual electro-Fenton process, in which H_2O_2 is electrochemically produced in situ through the cathodic reduction of dissolved oxygen expressed as Eq. (19)–(21), while Fe^{2+} is added externally, initiating the Fenton reaction given by Eq. (1) and regenerated by cathodic reduction as shown in Eq. (22) (Gümüş and Akbal, 2016; Moreira et al., 2017; Nidheesh et al., 2018).

$$O_2 + 2H^+ + 2e^- \rightarrow H_2O_2 \quad (19)$$

$$H_2O \rightarrow {}^{\bullet}OH + H^+ + e^- \quad (20)$$

$$2H_2O \rightarrow O_2 + 4H^+ + 4e^- \quad (21)$$

$$Fe^{2+} + H_2O_2 \rightarrow Fe^{3+} + {}^{\bullet}OH + OH^- \quad (1)$$

$$Fe^{3+} + e^- \rightarrow Fe^{2+} \quad (22)$$

This technology mitigates the costs and risks associated with H_2O_2 handling and reduces the initial Fe^{2+} input and sludge production (Zhang et al., 2019). TOC removal of 83% from paper mill wastewater was achieved by Klidi et al. (2019), after 12 h of this treatment with a modified carbon felt cathode and Ti/IrO_2-Ta_2O_5 anode, under 20 mA·cm^{-2} and pH = 3.

(ii) Type II is known as peroxi-coagulation, in which H_2O_2 is produced electrochemically in situ given by Eq. (19)–(21), while Fe^{2+} is produced in situ through the oxidation of a sacrificial iron anode as shown in Eq. (23).

$$Fe^0 \rightarrow Fe^{2+} + 2e^- \quad (23)$$

Ferric ions accumulate in the aqueous medium with the increase in electrolysis time, leading to $Fe(OH)_3$ precipitation; however, the use of electricity can reduce its quantity. Thus, in this type, pollutants are degraded by oxidation and coagulation, but the sludge are untreated (Casado, 2019; Gümüş and Akbal, 2016; Moreira et al., 2017; Nidheesh et al., 2018).

This type of electro-Fenton process has been applied successfully to treat textile wastewater, using a cylindrical reactor comprising an iron anode surrounded by a carbon felt cathode, a current intensity of 300 mA, and a pH of 3, achieving 71.1 % COD and 80 % color removal, and a two-fold BOD_5/COD ratio increase after 120 min (Ghanbari and Moradi, 2015).

(iii) Type III, that is, Fered-Fenton, in which both H_2O_2 and Fe^{2+} are externally added, Fe^{3+} is reduced to Fe^{2+} in the cathode, according to Eq. (22) (Gümüş and Akbal, 2016; Moreira et al., 2017; Nidheesh et al., 2018; Wang et al., 2016).

Zhang et al. (2012) recorded COD removal of 86.4 % from landfill leachate after treatment with 340 mM H_2O_2 and 28.33 mM Fe^{2+} for 120 min using an electrolytic cell with a Ti/RuO_2–IrO_2 anode and stainless steel cathode, at a current density of 19.2 mA·cm^{-2} and pH of 3.

(iv) Type IV refers to electrochemical peroxidation, wherein H_2O_2 is externally added while Fe^{2+} is produced in situ (Gümüş and Akbal, 2016; Moreira et al., 2017; Wang et al., 2016). Applying this method, Altin et al. (2017) obtained 91.7 % COD removal from pulp mill

wastewater after 20 min, under 1.0 A, pH = 3, 29.41 mM H_2O_2 supply, and cast-iron anode as the sacrificial catalyst source. Dealing with tissue paper wastewater, Un et al. (2015) recorded 81 % COD removal after 60 min, using an iron reactor operating as cathode and an iron anode in the center, at 20 $mA \cdot cm^{-2}$, pH = 2, and 200 mM H_2O_2 supply.

Recently, a novel electrochemical reaction system, the 3-D electro-Fenton system, has been explored. It is based on the packing of certain particles between two-dimensional electrodes, leading to an increase in efficiency due to (i) a much larger specific surface area of the 3-D electrodes; (ii) shorter distance between reactants and electrodes, improving mass transfer efficiency; and (iii) larger area-volume ratio and higher space utilization of the electrochemical reactor (Zhang et al., 2019).

The effects and optimized levels of each operating condition (electrode composition and distance, pH, temperature (T), $[H_2O_2]/[Fe^{2+}]$ when externally added, electric current, and air or O_2 supply) have been extensively studied over the last few years (Casado, 2019; Ganiyu et al., 2018; He and Zhou, 2017; Nidheesh and Gandhimathi, 2012; Ramos et al., 2019; Sevimli et al., 2014; Wang et al., 2010; Zhang et al., 2019).

4.3. Sono-Fenton process

When ultrasound waves are applied to a liquid, acoustic cavitation occurs, that is, the formation, growth, and collapse of microbubbles filled with vapor and/or gas (Babuponnusami and Muthukumar, 2014; Miklos et al., 2018). The rapid collapse of cavitation bubbles produces local temperature and pressure peaks, leading to decomposition of organics either by direct pyrolytic cleavage inside the cavitation bubble or by oxidation through •OH, •H, $•O_2H$, or H_2O_2 resulting from the gas phase pyrolysis of water, according to Eq. (12) and (24)–(28), in which “))” represents ultrasonic irradiation (Eskelinen et al., 2010; Miklos et al., 2018; Wang et al., 2016). Therefore, the reaction occurs inside the cavitation bubble, in the interfacial region between the bubble and the liquid phase, and in the bulk liquid (Babuponnusami and Muthukumar, 2014). In addition to the production of extra radicals, other advantages of coupling ultrasound with the Fenton process are improved mixing and contact between •OH and pollutants (due to high turbulence caused by the collapse of cavitation bubbles), enhanced ferrous ion regeneration

[Eq. (28)], and a clean and reactive surface for a heterogeneous catalyst (Adityosulindro et al., 2017; Kakavandi and Ahmadi, 2019; Rahmani et al., 2019).

$$H_2O \xrightarrow{))} {}^{\bullet}OH + H \quad (24)$$

$$O + H_2O \rightarrow 2{}^{\bullet}OH \quad (25)$$

$$2{}^{\bullet}OH \rightarrow H_2O_2 \quad (12)$$

$$H_2O_2 \xrightarrow{))} 2{}^{\bullet}OH \quad (26)$$

$$H_2O_2 + O_2 \xrightarrow{))} 2{}^{\bullet}O_2H \quad (27)$$

$$Fe - O_2H^{2+} \xrightarrow{))} Fe^{2+} + {}^{\bullet}O_2H \quad (28)$$

Recently, Rahmani et al. (2019) demonstrated the effectiveness of the sono-Fenton process in treating sludge from a poulter slaughterhouse wastewater treatment plant, removing 77 % COD after 60 min under the following operating conditions: 130 mM H_2O_2, 2.0 mM Fe^{2+}, pH = 3.0, and 40 kHz ultrasound irradiation. Siddique et al. (2014) also studied the synergistic effect between ultrasound and the Fenton process, employing a 200 W 20 kHz (Sonic Systems, Inc.) ultrasonic generator. A 78 % elimination of Reactive Blue 19 was achieved through this process, while only 50 % was obtained using the homogeneous conventional Fenton process.

Despite exhibiting some notable features and advantages, the technology required for full-scale application of sono-Fenton is still in an early development stage; therefore, it is not as well established as the other options (Miklos et al., 2018; Poyatos et al., 2010).

4.4. Combinations and hybrid Fenton processes

The combination of AOPs increases the efficiency of the overall process owing to the increased production of reactive oxygen species (i.e., cumulative effect) and/or positive interactions among the individual processes (i.e., synergistic effect) (Dewil et al., 2017). The most common combination of processes in wastewater treatment is the coupling of AOPs with biological treatment. Seibert et al. (2019) combined a 45 min photo-electro-Fenton (PEF) and 24 h aerobic biological treatment to treat landfill leachate, achieving removal of COD, BOD_5, SS, color and aromatic content of 68.0 %, 30.2 %, 26.3 %, 92.4 % and 89.2 %, respectively, under the following conditions: current intensity of 2.3 A, two 13 W UV lamps, 264.7 mM H_2O_2, 1.07 mM Fe^{2+} and pH ranging 3.5–4.5.

However, hybrid methods such as PEF may not be economically viable techniques for degrading large volumes of wastewater, as these additions to the Fenton process involve significant electricity costs, which may or may not compensate for the lower consumption of chemicals (Babuponnusami and Muthukumar, 2014; Casado, 2019; Moussavi and Aghanejad, 2014). Moreover, these processes do not prevent the continuous wastage of the catalyst. Even in the electro-Fenton process, where iron can be electro-generated, the catalyst is continuously lost at the expense of the sacrificial anode material. This limitation justifies the increasing focus laid recently on catalyst recovery/regeneration techniques, discussed in Section 5, and particularly in developing heterogeneous Fenton catalysts, presented in Section 6.

Table 2. Compilation of results reported on the application of modified homogeneous Fenton process to real industrial wastewater treatment.

Operating conditions	Wastewater treated	Parameter	Removal (%)	Ref.	Notes
$[H_2O_2]$ = 29.41 mM; $[Fe^{2+}]$ = 0 mM (electrogenerated); pH = 2.5; t = 20 min; T = ambient; Two pairs of cast iron cathode and anode, 1 cm apart; Current intensity = 1.0 A	Pulp and paper mill wastewater	COD	91.7	Altin et al. (2017)	Electro-Fenton
$[H_2O_2]$ = 88.24 mM; $[Fe^{3+}]$ = 17.91 mM; pH = 6.9; t = 60 min; T = 25 ºC; 24-30 kHz ultrasonic irradiation	Pulp bleaching wastewater	COD	12.0	Eskelinen et al. (2010)	Sono-Fenton-like
$[H_2O_2]$ = 88.24 mM; $[Fe^{3+}]$ = 17.91 mM; pH = 6.9; t = 60 min; T = 25 ºC; 12 mW·cm^{-2} UV	Pulp bleaching wastewater	COD	20.0	Eskelinen et al. (2010)	Photo-Fenton-like
$[H_2O_2]$ = 41 mM; $[Fe^{2+}]$ = 0.18 mM; pH = 2.8; t = 360 min; T = 25 ºC; 19 kJ·L^{-1} solar irradiation	Pulp mill wastewater	DOC	90.0	Fernandes et al. (2014)	Solar-photo-Fenton After anaerobic digestion and yeast treatment
$[H_2O_2]$ = 35.1 mM; $[Fe^{2+}]$ = 3.51 mM; pH = 2.8; T = 25 ºC; 450 W UV lamp	Reverse osmosis retentate from a paper mill	TOC	≈ 100	Hermosilla et al. (2012)	Photo-Fenton
		COD	≈ 100		
$[H_2O_2]$ = 0 mM (electrogenerated); $[Fe^{2+}]$ = 0.5 mM; pH = 3.0; t = 12 h; T = ambient; Commercial DSA anode (Ti/IrO_2-Ta_2O_5) and modified carbon felt cathode; Current density = 20 mA·cm^{-2}	Paper mill wastewater	TOC	83.0	Klidi et al. (2019)	Electro-Fenton TOC removal increased to 91 % upon addition of 1 g·L^{-1} NaCl
$[H_2O_2]$ = 50 mM; $[Fe^{2+}]$ = 0.09 mM; pH = 2.8; t = 250 min; T = ambient; 31 kJ·/L^{-1} solar irradiation	Pulp mill wastewater	DOC	90.0	Lucas et al. (2012)	Solar-photo-Fenton After biological treatment
$[H_2O_2]$ = 15 mM; $[Fe^{2+}]$ = 0 mM (electrogenerated); pH = 4.0; t = 30 min; T = ambient; Tinplate sheet cathode and anode, 2 cm apart; Current density = 5 mA·cm^{-2}	Paper recycling plant wastewater	COD	95.7	Moussavi and Aghanejad (2014)	Electro-Fenton
		BOD_5/COD	0.12 to 0.43		
$[H_2O_2]$ = 29.41 mM; $[Fe^{2+}]$ = 0.179 mM; pH = 3.0; t = 120 min; T = ambient; 475 W·m^{-2} solar irradiation	Kraft pulp (final) wastewater	AOX	19.1	Rabelo et al. (2014)	Solar-photo-Fenton
		TOC	24.4		
		COD	61.8		
		BOD_5	45.8		
		BOD_5/COD	0.40 to 0.57		
$[H_2O_2]$ = 178 mM; $[Fe^{2+}]$ = 1.0 mM; pH= 2.0; t = 10 min; T = 60 ºC; 150 W UV lamp	Pulp bleaching wastewater	AOX	89.4	Ribeiro et al. (2020b)	Photo-Fenton
		COD	20.0		
		BOD_5/COD	0.05 to 0.09		
		Color	76.0		
$[H_2O_2]$ = 44.11 mM; $[Fe^{2+}]$ = 0 mM (electrogenerated); pH = 3.0; t = 45 min; T = 24 ºC; Cast iron cathode and anode, 7 cm apart; Current intensity = 1.0 A	Pulp bleaching wastewater	COD	54.9	Sevimli et al. (2014)	Electro-Fenton
$[H_2O_2]$ = 200 mM; $[Fe^{2+}]$ = 0 mM; pH = 2.0; t = 60 min; T = ambient; Iron reactor operating as cathode, iron anode in the center; Current density = 20 mA·cm^{-2}	(Tissue) Paper wastewater	COD	81.0	Un et al. (2015)	Electro-Fenton
$[H_2O_2]$ = 14.71 mM; $[Fe^{2+}]$ = 0 mM (electrogenerated); pH = 3.0; t = 40 min; T = ambient; Cast iron cathode and anode, 2 cm apart; Current intensity = 200 mA	Textile wastewater	COD	82.1	Ghanbary and Moradi (2015)	Electro-Fenton
		BOD_5/COD	0.14 to 0.34		
		Color	94.0		
$[H_2O_2]$ = 0 mM (electrogenerated); $[Fe^{2+}]$ = 3 mM; pH = 3.0; t = 160 min; T = ambient; Pt anode surrounded by a graphite felt cathode; Current intensity = 300 mA	Textile wastewater	COD	64.2	Ghanbary and Moradi (2015)	Electro-Fenton 2 L_{Air}·min^{-1} supply
		BOD_5/COD	0.14 to 0.36		
		Color	77.0		
$[H_2O_2]$ = 0 mM (electrogenerated); $[Fe^{2+}]$ = 0 mM (electrogenerated; pH = 3.0; t = 120 min; T = ambient; Iron anode surrounded by a graphite felt cathode; Current intensity = 300 mA	Textile wastewater	COD	71.1	Ghanbary and Moradi (2015)	Electro-Fenton 2 L_{Air}·min^{-1} supply
		BOD_5/COD	0.14 to 0.32		
$[H_2O_2]$ = 73.5 mM; $[Fe^{2+}]$ = 1.79 mM; pH = 3.0; t = 120 min; T = 25 ºC; 6 W UV lamp (1.38x10^{-9} Einstein·s^{-1})	Textile wastewater	TOC	70.4	Torrades and Montaño (2014)	Photo-Fenton
		COD	76.3		
$[H_2O_2]$ = 0 mM (electrogenerated); $[Fe^{2+}]$ = 2 mM; pH = 3.0; t = 240 min; T = 20 ºC; Pt wire anode, placed in the center of a hollow cylindrical cathode of PAN-based activated carbon fiber cloth; Current density = 3.2 mA·cm^{-2}	Textile (dyeing) wastewater	COD	75.2	Wang et al. (2010)	Electro-Fenton 0.15 L_{O2}·min^{-1} supply

Table 2 (cont.). Compilation of results reported on the application of modified homogeneous Fenton process to real industrial wastewater treatment.

Operating conditions	Wastewater treated	Parameter	Removal (%)	Ref.	Notes
$[H_2O_2]$ = 58.82 mM; $[Fe^{2+}]$ = 0 mM (electrogenerated); pH = 3.0; t = 20 min; T = ambient; Two pairs of cast iron cathode and anode, 1 cm apart; Current intensity = 2.0 A	Landfill leachate	COD	72.0	Atmaca (2009)	Electro-Fenton
		Color	90.0		
		Phosphate	87.0		
$[H_2O_2]$ = 75 mM; $[Fe^{2+}]$ = 50 mM; pH = 2.5; t = 60 min; T = 25 ºC; 450 W UV lamp	Landfill Leachate	COD	70.0	Hermosilla et al. (2009)	Photo-Fenton
$[H_2O_2]/[Fe^{2+}]$ = 1 (externally added); pH = 3.0; t = 43 min; T = 28 ºC; Aluminum cathode and anode, 3 cm apart; Current density = 49 $mA \cdot cm^{-2}$	Landfill leachate	COD	94.0	Mohajeri et al. (2010)	Electro-Fenton
		Color	95.8		
$[H_2O_2]$ = 264.7 mM; $[Fe^{2+}]$ = 1.07 mM; pH = 3.5 – 4.5; t = 45 min; T = ambient; two 13 W UV lamps; two pairs of cast iron cathode and anode, 2 cm apart; Current intensity = 2.3 A	Landfill leachate	COD	68.0	Seibert et al. (2019)	Photo-electro-Fenton
		BOD_5	30.2		
		BOD_5/COD	0.18 to 0.40		
		Color	92.4		
		SS	26.3		
		Aromatics	89.2		
$[H_2O_2]$ = 340 mM; $[Fe^{2+}]$ = 28.33 mM; pH = 3.0; t = 120 min; T = ambient; Stainless steel cathode and Ti/RuO_2–IrO_2 anode, 2.1 cm apart; Current density = 19.2 $mA \cdot cm^{-2}$	Landfill leachate	COD	86.4	Zhang et al. (2012)	Electro-Fenton
$[H_2O_2]$ = 0 mM (electrogenerated); $[Fe^{2+}]$ = 0.6 mM; pH = 4.0; t = 1.8 h; T = ambient; Titanium anode, activated carbon fibre cathode, 5 cm apart; Current density = 3.7 $mA \cdot cm^{-2}$	Coking wastewater	COD	55.8	Zhu et al. (2011)	Electro-Fenton After anaerobic treatment
$[H_2O_2]$ = 0 mM (electrogenerated); $[Fe^{2+}]$ = 1.79 mM; pH = 3.0; t = 380 min; T = ambient; BDD anode surrounded by a carbon felt cathode 0.12 L/min O2 supply); Current density = 300 mA	Photographic processing wastewater	TOC	85.0 - 90.0	Bensalah et al. (2013)	Electro-Fenton 0.12 $L_{O2} \cdot min^{-1}$ supply
		Phenol	100		
$[H_2O_2]$ = 88.24 mM; $[Fe^{2+}]$ = 3.58 mM; pH = 7.8; t = 50 min; T = ambient; 40 W UV lamp	Photographic processing wastewater	TOC	85.0 - 90.0	Bensalah et al. (2013)	Photo-Fenton
$[H_2O_2]$ = 76.1 mM; $[Fe^{2+}]$ = 1.07 mM; pH = 2.8; t = 20 days; T = ambient; 13.6 $kJ \cdot L^{-1}$ solar irradiation	Cork boiling wastewater	COD	65.0 – 75.0	Pintor et al. (2011)	Solar photo-Fenton H_2O_2 supplied in recirculated cork bleaching wastewater
		BOD_5	47.0 – 63.0		
		BOD_5/COD	0.18 to 0.28		
		DOC	70.0 – 75.0		
		Phenol	78.0 – 83.0		
		Aromatics	89.0 – 91.0		
$[H_2O_2]$ = 77.1 mM; $[Fe^{2+}]$ = 0.358 mM; pH = 2.8; t = Until maximum removal; T = ambient; 31.5 $kJ \cdot L^{-1}$ solar irradiation	Cork bleaching wastewater	DOC	94.0	Vilar et al. (2009)	Solar-photo-Fenton
$[H_2O_2]$ = 130 mM; $[Fe^{2+}]$ = 2.0 mM; pH = 3.0; t = 60 min; T = ambient; 40 kHz ultrasound	Activated sludge from poulter slaughterhouse wastewater treatment plant	COD	77.0	Rahmani et al. (2019)	Sono-Fenton

5. Regeneration and reuse of catalyst

One strategy to overcome the problem of catalyst loss and consequent iron sludge generation is catalyst regeneration and/or reuse. The cheapest and easiest method of achieving this is to acidify the sludge to pH < 2.0, resolubilize the precipitated iron, and directly reuse it in the Fenton treatment. The supplied iron would be essentially Fe^{3+}, with the known disadvantages of lower initial efficiency compared to Fe^{2+} and a higher tendency to form complexes with carboxylic acids (Fernandes et al., 2014). This approach was demonstrated by Bolobajev et al. (2014), who treated three types of industrial wastewater by the Fenton process, using iron sludge as a catalyst after precipitation and centrifugation. The COD and DOC removal were

similar after four treatment cycles employing the reused iron-containing sludge, thereby proving the efficiency of this catalyst (Table 3). The loss of iron sludge between cycles due to precipitation/separation processes was recorded as 5–10 % per cycle, which may be solved using an additional amount of iron salt at the beginning of each cycle to ensure equal initial iron concentration.

Cao et al. (2009) introduced a regeneration method to prevent the accumulation of organics in the regenerated iron catalyst, including sludge dewatering, drying at 105 °C, baking at 400 °C, and dissolving in H_2SO_4 to a pH < 2. The obtained regenerated sludge was used in the Fenton treatment of fine chemical wastewater (10 mM H_2O_2; 1 mM Fe^{2+} from the sludge; pH = 3; and treatment time, t = 200 min), achieving approximately 65 % COD removal over six reuse cycles.

Lal and Garg (2017) studied the possibility of employing coagulation with $FeCl_3$ as a pre-treatment to the Fenton process using dissolved ferric ions as Fenton catalysts for lignin and TOC removal from (synthetic) pulp wastewater. In their experiment, 2 g $FeCl_3 \cdot L^{-1}$ was used for coagulation, after which 275 $mg \cdot L^{-1}$ of dissolved iron remained in solution (Fe^{3+} accounting for 258 $mg \cdot L^{-1}$). The dissolved iron functioned as an effective Fenton-like catalyst, removing 85 % lignin and 48 % TOC within 30 min, using 98 mM H_2O_2 (pH = 4).

An important step in such methodologies is the location and time at which the sludge separation/regeneration operations should be incorporated in a treatment system. Kishimoto et al. (2013) studied the performance of two sludge separation methods within the electro-Fenton process: sequential and separation batch modes. In the sequential batch mode, electro-Fenton reaction, pH neutralization, sludge sedimentation, and sludge re-dissolution occurred successively in the same reactor; in the separation batch mode, electro-Fenton treated wastewater passed through a second reactor, where pH neutralization and sludge sedimentation occurred. Then, sludge was reintroduced into the electro-Fenton reactor, where it was re-dissolved before the next treatment cycle. The results showed that the separation batch mode was the most efficient (100 % iron recovery) owing to the formation of insoluble iron oxide. According to the authors, the reuse of iron sludge can decrease the chemical cost by 96 % (Kishimoto et al., 2013).

Zhang et al. (2017) used Fenton sludge as an iron source for the synthesis of nickel ferrite ($NiFe_2O_4$), which in turn was used as the Fenton catalyst for phenol degradation, in the initial

step in real wastewater treatment. The catalyst was synthesized by adding $Ni(NO_3)_2$ to the Fenton sludge (Fe:Ni molar ratio of 2:1), followed by dropwise addition of NaOH, washing, and sintering of the resultant product at 800 °C. The obtained $NiFe_2O_4$ was then used as the Fenton catalyst (2 $g \cdot L^{-1}$, in the presence of 120 mM H_2O_2), removing approximately 95.0 % phenol and 94.4 % TOC after 330 min, with approximately 6.3 % of the total iron leached into the solution (pH = 3). The recovery of the solid catalyst after the reaction was approximately 97 %.

Another technique for iron recovery from treated wastewater is ion exchange (IE), a simple, low-cost technology that is recognized as an alternative for the removal or recovery of inorganic pollutants, particularly heavy metals (Martins et al., 2017). Víctor-Ortega et al. (2016) utilized two IE resins (strong-acid cation exchange and weak-base anion exchange resins) to recover iron from olive mill wastewater. The apparatus included two acrylic columns filled with resins, operating in series through recirculation or continuous mode. Equilibrium was reached after approximately 20 min in continuous mode, with the wastewater passing through two IE columns, the first with the strong-acid cation exchange resin, and the second with the weak-base anion exchange resin. Under this configuration, 20 $g \cdot L^{-1}$ and 30 $g \cdot L^{-1}$ for the cationic and anionic resins, respectively, were the minimum dosages to ensure an ion removal efficiency over 90 %. Reis et al. (2018) integrated IE with the Fenton process for COD removal from real olive mill wastewater; The commercial resin Lewatit TP 207 was used, and for dosage above 40 $g \cdot L^{-1}$, approximately 90 % iron was removed from the wastewater after treatment with the Fenton process under optimized conditions (735 mM H_2O_2; 0.90 mM Fe^{2+}; pH = 3.5; t = 60 min, T = 25 °C). According to the authors, the loaded resin can be regenerated using a 1.5 M H_2SO_4 solution, rendering it effective for multiple adsorption/desorption cycles, as the iron removed from the resin was reutilized in the Fenton process.

A different approach to tackle catalyst wastage is by adding a reducing agent, such as hydroxylamine (NH_2OH), to regenerate Fe^{2+} from Fe^{3+} in situ during the Fenton treatment. The generation of ferrous ions in the presence of NH_2OH occurs according to Eq. (29)–(31) (Lal and Garg, 2017):

$$Fe^{3+} + NH_2OH \rightarrow NH_2O^{\bullet} + Fe^{2+} + H^+ \quad (29)$$

$$Fe^{3+} + NH_2O^{\bullet} \rightarrow NHO + Fe^{2+} + H^+ \quad (30)$$

$$5Fe^{3+} + 2H_2O + NH_2O^{\bullet} \rightarrow NO_3^- + 5Fe^{2+} + 6H^+ \quad (31)$$

Lal and Garg (2017) used ferric ions from coagulation as Fenton catalyst and adding NH_2OH to the system increased TOC removal from 48 % to approximately 56 % after 30 min. Fayazi et al. (2016) added NH_2OH in the Fenton-like removal of methylene blue dye from wastewater, using 12 mM H_2O_2 and 2.0 $g \cdot L^{-1}$ of a magnetically activated carbon/maghemite (AC/γ-Fe_2O_3) catalyst. After 40 min, the addition of 2 mM NH_2OH (hydroxylamine) increased the dye removal from 50 % to approximately 100 %. Moreover, if the NH_2OH concentration was increased to 6 mM, the same result was obtained after 10 min. He et al. (2020) added NH_2OH to the Fenton process to degrade benzoic acid. The addition of 0.2 mM NH_2OH increased the degradation from 25.3 % to 81.3 % after 20 min, at pH = 3, with 0.4 mM H_2O_2, and 0.01 mM Fe^{2+}. The benzoic acid was significantly degraded even at pH 5. Moreover, only approximately 30 % of Fe^{2+} was converted to Fe^{3+}, indicating the effectiveness of NH_2OH in catalyst recovery. It must be stated that NH_2OH is toxic, which severely limits its full-scale application; hence, research focused on mitigating its toxic effects and studying its end-products should be conducted. The entrapment of NH_2OH in specific solid matrices could effectively minimize this hazard, limiting the leaching of toxic compounds.

Another method to increase Fe^{2+} performance during the reaction involves the addition of a chelating agent (L). Ahile et al. (2020) reported that the major advantages of this technique are the increased solubility of nonpolar and lipophilic pollutants, and enhanced dissolution of iron in a wider pH range than conventional Fenton processes. In the photo-Fenton process, chelates with higher quantum yields can be obtained from •OH compared to other Fe (III)-complexes, facilitating the application of a wider spectrum of solar radiation. A suitable chelating agent must be used to provide more than two appropriate functional groups, whose donor atoms can donate a pair of electrons to a metal atom. Furthermore, the functional groups must form a ring between the metal atoms and the chelating agent L (Zhang and Zhou, 2019). The biodegradability and the increase in toxicity due to the formation of heavy metal complexes, as well as the stability constant of the complex, must also be considered when selecting a chelating agent.

This technique was used by De Luca et al. (2014) to obtain a feasible photo-Fenton method at neutral pH. The authors achieved improved results using EDTA and NTA as chelating agents,

which formed photoactive species $Fe^{3+}L$ that maintained the solubility of iron. Using Fe(III)-EDTA and Fe(III)-NTA chelates at neutral pH, sulfamethoxazole removal of 77.3 % after 75 min and 82.2 % after 120 min, respectively, were attained. The authors identified two drawbacks: (i) EDTA and NTA are only slightly soluble in acidic water, thus, this method cannot be applied for the entire pH range; (ii) •OH reacts with both sulfamethoxazole and chelate, cleaving complexes and releasing iron to the solution, thereby limiting catalytic activity. Ye et al. (2020) used EDDS in the PEF process to treat pharmaceutical fluoxetine from urban wastewater at circumneutral pH. The use of an IrO_2/air diffusion cell at 50 mA with 0.20 mM of catalytic complex Fe(III)-EDDS (1:1) achieved the complete removal of fluoxetine in 60 min, exhibiting better performance than uncomplexed Fe(III). This was due to the higher amount of Fe^{2+} formed during Fe(III)-EDDS photo-reduction, causing higher •OH production.

Despite promising advances in catalyst regeneration techniques, the unsolved drawbacks associated with such methods have led to the recent research for the development of effective, safe, and low-cost heterogeneous Fenton catalysts, as a cutting-edge technique to overcome the iron wastage issue. Section 6 presents the primary outcomes of these investigations.

6. Heterogeneous Fenton process

Generally, the heterogeneous Fenton process has the same principles as the homogeneous process. However, the •OH production is catalyzed on the surface of the heterogeneous material, represented by “X” in Eq. (32) – (33). Thus, in addition to Fenton chemistry, adsorption of reactant molecules occurs at the active sites of the catalyst surface. At the end of the reaction, the product molecules are desorbed and the active sites are available to bind with other reactant molecules (Garcia-Segura et al., 2016; Queirós et al., 2015; Sreeja and Sosamony, 2016). The Fenton reaction rate at the interface increases with increasing catalyst surface area and porosity (Vorontsov, 2019).

$$X - Fe^{2+} + H_2O_2 \rightarrow X - Fe^{3+} + {}^{\bullet}OH + OH^- \quad (32)$$

$$Fe^{3+} + H_2O_2 \rightarrow X - Fe^{2+} + {}^{\bullet}O_2H + H^+ \quad (33)$$

An ideal catalyst has suitable characteristics, such as high activity and selectivity for •OH generation, large surface area, high porosity, physical-chemical stability (including low

leaching), homogeneity, resistance to poisoning and attrition, non-selectivity in most cases, and low cost (Poyatos et al., 2010; Poza-Nogueiras et al., 2018; Wang et al., 2016).

Regardless of the heterogeneous nature of the Fenton catalyst, its recyclability is an important feature of such processes which is affected by the leaching of the active metal element to the solid catalyst surface, resulting in its deactivation (Wang et al., 2016). Iron leaching is not easily prevented because surface iron is extracted into the solution due to complexation with organic acids, which are formed during the oxidation of water pollutants. The leached iron exhibits the same catalytic activity as in the homogeneous Fenton process, with the highest performance at pH of approximately 3; increasing the pH should limit iron leaching, favoring catalytic activity throughout the active sites of the catalyst surface (Vorontsov, 2019; Wang et al., 2016).

The heterogeneous Fenton process has several advantages over the homogeneous process. It can be operated at a wide pH range, without neutralizing the treated wastewater; it mitigates the formation of iron sludge and associated issues/cost. The catalyst can be easily handled, safely stored, efficiently recovered by sedimentation, filtration, or magnetic separation, and reused. The reaction is not inhibited due to the concentration of inorganic carbonate (Bokare and Choi, 2014; Casado, 2019; Dulova et al., 2011; Poza-Nogueiras et al., 2018; Sreeja and Sosamony, 2016). Moreover, Rodríguez et al. (2016) also emphasized that heterogeneous Fenton may lead to 77 % reduction in the water footprint for treatments in factories and approximately 40 % for the final discharge in an urban wastewater treatment plant. However, the drawbacks of the process include high dosage of hydrogen peroxide (almost four times that of the homogenous system (Rodríguez et al., 2016)); slow kinetics, limited by mass transfer of H_2O_2 to the active sites on the catalyst surface and by the lower reaction between H_2O_2 and Fe^{3+}, in all iron-impregnated catalysts; and potential formation of catalyst agglomerates, reducing free surface availability; production cost of the solid catalyst, which increases with increasing catalyst loading (Bokare and Choi, 2014; Garcia-Segura et al., 2016; Wang et al., 2016). Therefore, the choice of materials and operating conditions in the heterogeneous Fenton process are of utmost relevance. In the following sections, different catalyst materials have been reviewed. Table 3 presents the major outcomes of the application of the heterogeneous Fenton process to real wastewater.

6.1 Zero-valent state metal catalyst

The Fenton process can be easily modified using zero-valent iron (ZVI or Fe^0) as a heterogeneous catalyst, that has several advantages, such as low toxicity and cost, high reactivity in •OH generation, easy separation from the liquid after treatment, and decreased leaching of iron into the treated wastewater (Bokare and Choi, 2014; Dulova et al., 2011).
Its versatility is exhibited in the complexity of the reaction mechanism of ZVI, involving oxidation, reduction, coprecipitation, surface adsorption, etc., which varies according to the contaminants it reacts with (Thomas et al., 2021).
At acidic conditions, the surface layer of the Fe^0 particles oxidizes causing in-situ production of Fe^{2+}, initiating ZVI-catalyzed heterogeneous Fenton chemistry, according to Eq. (34)–(37) (Segura et al., 2013; Sevimli et al., 2014). As Fe^0 should be solubilized to catalyze the reaction with H_2O_2, maintaining a constant acidic pH is very important for the oxidation of pollutants in wastewater (Sevimli et al., 2014). Moreover, increasing the pH may cause ferric oxyhydroxide accumulation on the metal surface, resulting in surface passivation and loss of reactivity (Babuponnusami and Muthukumar, 2014; Bokare and Choi, 2014).

$$Fe^0 + 2H^+ \rightarrow Fe^{2+} + H_2 \quad (34)$$

$$Fe^0 + O_2 + 2H^+ \rightarrow Fe^{2+} + H_2O_2 \quad (35)$$

$$2Fe^{3+} + Fe^0 \rightarrow 3Fe^{2+} \quad (36)$$

$$Fe^0 + H_2O_2 + 2H^+ \rightarrow Fe^{2+} + 2H_2O \quad (37)$$

Kallel et al. (2009) studied the COD removal from olive mill wastewater using ZVI as a Fenton catalyst, observing a three-stage degradation mechanism. (1) After adding iron, the reaction is slow due to the low production of Fe^{2+} from corroding iron metal, implying lower •OH generation. (2) When the optimum Fe^{2+} concentration is achieved, Fenton chemistry occurs and the degradation rate increases. (3) Fe^{2+} generation continues even after H_2O_2 depletion, indicated by the resurgence of color in the treated wastewater. Degradation of organics with the depletion of H_2O_2 occurs due to the oxidizing effect of ferryl ion species; Segura et al. (2013) reported that such species may be formed at approximately neutral pH and can act as oxidants when using ZVI as a Fenton catalyst in pharmaceutical wastewater treatment. This occurrence was supported by the fact that neutral pH values (5.3–5.5) were obtained as the reaction

progressed. This is consistent with Sevimli et al. (2014) who observed a gradual increase in the pH of pulp wastewater during the ZVI heterogeneous Fenton process. In that study, COD removal increased from 44.5 % in the conventional homogeneous Fenton process to 58.2 % with less than half the catalyst dosage, because of the efficient conversion of Fe^{3+} to Fe^{2+} at the metal surface.

In a study on picric acid degradation, Dulova et al. (2011) obtained approximately equal amounts of dissolved iron from ZVI after 30 min, compared to the homogeneous Fenton process with a catalyst dosage of 100 $mg \cdot L^{-1}$ (at pH = 3). This proves that, after the initial Fe^{2+} leaching, the organics primarily degrade through Fenton oxidation, though the adsorption onto the metal surface and subsequent in-situ oxidation by •OH may also contribute to the overall efficiency (approximately 7.5 %).

Furthermore, Ramos et al. (2020) estimated an operating cost of approximately 4.6 $USD \cdot m^{-3}$ using ZVI as Fenton catalyst for 90 % COD removal from textile industry.

An alternative to the most commonly studied ZVI is zero-valent aluminum (ZVAl), which provides a greater thermodynamic driving force for electron transfer than ZVI, and is lighter than Fe (Bokare and Choi, 2009, 2014). Reactions in the ZVAl/O_2 system start with the corrosive dissolution of the aluminum oxide layer on the catalyst surface, with reactions expressed in Eq. (38) – (39) and (11), leading to H_2O_2 formation. As Al^{3+} cannot act as the reducing agent for H_2O_2, the Fenton reaction does not occur; according to Bokare and Choi (2009), the possible mechanism of •OH generation is the direct electron transfer from Al^0 to H_2O_2 given by Eq. (40). The authors reported approximately 90 % degradation of 4-clorophenol after 275 min using 1 $g \cdot L^{-1}$ ZVAl at pH = 2, and in-situ H_2O_2 generation of approximately 0.1 mM.

$$Al^0 \rightarrow Al^{3+} + 3e^- \quad (38)$$

$$O_2 + H^+ + e^- \rightarrow {}^{\bullet}O_2H \quad (39)$$

$$2\,{}^{\bullet}O_2H \rightarrow H_2O_2 + O_2 \quad (11)$$

$$Al^0 + 3H_2O_2 \rightarrow Al^{3+} + 3\,{}^{\bullet}OH + 3OH^- \quad (40)$$

However, the surface Al_2O_3 layer is not easily degraded under neutral or near-neutral pH conditions, limiting the applications of ZVAl-based systems to pH < 4, such as Fe-based Fenton processes (Bokare and Choi, 2014).

6.2 Synthesized iron-supporting catalyst

The development in heterogeneous Fenton catalysis research is evident in the synthesis of iron-supporting catalysts. The iron in the synthesized catalyst may be obtained either from iron minerals or iron salts and is usually entrapped or impregnated in a solid support. Catalyst support has three primary functions, as summarized by Poyatos et al. (2010): (i) increasing the catalyst surface area; (ii) decreasing sintering and improving hydrophobicity, as well as the thermal, hydrolytic, and chemical stability of the catalyst; and (iii) governing the useful lifecycle of the catalyst. The suitability of the supports are determined by the following characteristics: high porosity, large surface area, high adsorption capacity facilitating degradation of organics, strong physicochemical adsorption of the iron particles without affecting their reactivity, ease of separation from the liquid, and chemical inertness (Babuponnusami and Muthukumar, 2014; Poyatos et al., 2010; Wang et al., 2016). The commonly used supports include zeolite, AC, clay, polymers, silica, fibers, and alumina (Poyatos et al., 2010; Wang et al., 2016).

Zeolites are hydrated aluminosilicate minerals, characterized by a highly crystalline SiO_2, and very high external surface area and cation exchange capacity (Poza-Nogueiras et al., 2018; Soon and Hameed, 2011). At least 41 types of natural zeolites are known to exist, and several others may be synthesized, particularly by reaction of sodium aluminate with sodium silicate. The catalysts can be obtained by impregnation of synthetic zeolite with ferric ions followed by calcination, or by IE of sodium in zeolite with ferric ions (Poza-Nogueiras et al., 2018; Soon and Hameed, 2011). A significant limitation of using common zeolites as supports is that their active sites are often highly selective to specific reactant and product molecules (Soon and Hameed, 2011). Aleksic et al. (2010) prepared the FeZSM5 zeolite catalyst from NH_4ZSM5 via solid-state IE under aerobic conditions, achieving an 37 $mg \cdot g^{-1}$ iron content in the zeolite, which is 10 times that in the original zeolite. The synthesized Fenton catalyst was utilized in the degradation of RB137 azo dye, with 58 % TOC removal achieved after 1 h using 1.49 $g \cdot L^{-1}$ of FeZSM5 and 10 mM of H_2O_2 at pH 5 and 25 °C. By adding UV irradiation to this system, 81.1 % TOC removal and complete decolorization were recorded under the same conditions, at pH 6. The authors also observed that the bulk iron concentration due to leaching from the zeolite support was 17 times lower than that in the homogeneous Fenton process. In another study on dye wastewater treatment (Orange II dye), color, TOC, and COD removal efficiencies of 91 %, 36 %, and 29 %,

respectively, were obtained after 90 min with 6 mM H_2O_2, at pH 3, and 70 °C, using commercial FeZSM5 zeolite as the catalyst (Queirós et al., 2015); the iron concentration in the treated solution was 0.173 mg·L^{-1}, corresponding to a leaching rate of 0.13 %.

Another well-addressed iron-supporting Fenton catalyst is the Fe-activated carbon (AC/Fe) catalyst. Carbon materials, synthetic or reutilized waste, can be activated by improving its porosity and increasing its surface area for a specific reaction (Soon and Hameed, 2011). Duarte et al. (2013) analyzed an iron-based Fenton catalyst supported on commercial AC for real textile wastewater treatment in a continuous packed-bed reactor. Activated carbon particles were wet-impregnated with iron (II) acetate solution, and then the particles were thermally treated (2 h at 300 °C in a He stream) to obtain the AC/Fe catalyst with 7 wt. % Fe. Using 30 mM H_2O_2, at pH 2.5 and a catalyst/wastewater inflow ratio of 3.3 g catalyst·min·mL^{-1}, removal of 96.7, 73.6, 66.3, and 72.5 % of color, TOC, COD, and BOD_5, respectively, was achieved at hydraulic retention time of 22.5 min. The authors also reported very low iron leaching, with only 1.25 % of the initial Fe load lost after 60 h of continuous operation. Fayazi et al. (2016) achieved complete degradation of methylene blue dye after 40 min of heterogeneous Fenton treatment in the presence of 4 mM NH_2OH with 12 mM H_2O_2, at pH 5, and 2 g·L^{-1} of a catalyst with 71.3 wt. % iron content; the catalyst was prepared by impregnating AC with maghemite via coprecipitation of $FeCl_3$ and $FeSO_4$ on oxidized AC at room temperature. 85 % degradation was obtained even after seven consecutive cycles, with a maximum iron leaching of 1.1 mg·g^{-1}, establishing the stability and reusability of the catalyst. Lan et al. (2015) impregnated AC fibers with $Fe(NO_3)_3$ and calcinated it at 500 °C for 2 h in argon flow to obtain an AC/Fe_2O_3 catalyst with 1.2 % wt. Fe, and a significantly high surface area of 1237 m^2·g^{-1}. This catalyst was used in the photo-Fenton degradation of acid red B dye, and complete removal was achieved under optimized conditions, with negligible loss of activity after four consecutive cycles and low iron leaching.

Clays are another category of effective catalyst supports because of their abundance in nature, ease of customization for specific applications, catalytic activity over a wide pH range (3.0–9.5), and high reuse efficiency, though they require pretreatment before use (Soon and Hameed, 2011). A bentonite/Fe catalyst was prepared by Gao et al. (2015) by adding bentonite to a mixture of sodium carbonate and ferric nitrate, and ageing it at 60 °C for 1 d. Subsequently, the

precipitate was separated and dried overnight to obtain the catalyst, which had approximately four times the surface area and 1.5 times the pore volume of raw bentonite. Almost complete degradation of rhodamine-B was attained by heterogeneous photo-Fenton process after 300 min of reaction at pH 4.2, using 0.25 $g \cdot L^{-1}$ of Bentonite/Fe catalyst and 12 mM H_2O_2. The authors verified that rhodamine-B removal occurred due to the equal rate of degradation and adsorption, and that the synthesized catalyst could be reutilized in five consecutive cycles, without loss of catalytic activity, and with only 0.48 $mg \cdot L^{-1}$ iron leaching. In another study (Guo et al., 2014) using clays as the iron-supporting catalyst, kaolin/Fe was prepared using a technique similar to Gao et al. (2015) and it was employed for the photo-Fenton degradation of rhodamine-B. In addition to achieving 98 % discoloration and 66 % mineralization of rhodamine-B, the study presented certain notable conclusions regarding the kaolin/Fe catalyst, such as the high activity over pH ranging 2.21–10.13, ease of separation using a simple precipitation process, and unaltered performance even after five cycles, with negligible iron leaching. Natural polymers are another suitable choice as catalyst supports. The disadvantage of using such materials is their higher selectivity and lower catalytic activity compared to other materials; hence, further research in this field is required (Soon and Hameed, 2011). Chagas et al. (2019) incorporated Fe^{2+} into soluble chitosan gel (CT), usually used for chromium (Cr) adsorption; the composite material containing structurally immobilized Cr (CT/Fe/Cr) was used as the Fenton catalyst for the degradation of methylene blue dye, achieving 93.8 % degradation under optimal conditions. After six cycles, the degradation decreased to approximately 70 %, and the catalyst was rinsed with ethanol, improving the degradation in the next cycle to approximately 80 %. Another relevant result of that study was that the hemolytic potential of the treated wastewater was always below the 5 % limit, indicating limited toxicity of Cr released to the environment. Melero et al. (2009) co-condensed $FeCl_3$ and tetraethoxysilicate to support iron oxide Fe_2O_3 onto an SBA-15 silica mesostructured material (SBA-15/Fe_2O_3), which was then successfully applied as a Fenton catalyst to treat pharmaceutical wastewater in a continuous fixed-bed reactor. Under optimized conditions, 59% TOC and 81 % COD removal were obtained, with BOD_5/COD increasing from 0.20 to 0.30 (Melero et al., 2009). Su et al. (2011) investigated the treatment of textile wastewater (86.7 % COD and 96.6 % color removal under optimized conditions) using the fluidized-bed Fenton process, where Fe^{3+} produced in the Fenton reaction

is converted to iron oxide on the surface of SiO_2 carriers through crystallization or sedimentation. This prevents catalyst agglomeration, improves kinetics by overcoming mass transfer limitations due to catalyst fluidization, and reduces sludge production (Garcia-Segura et al., 2016). The iron oxide immobilized on the SiO_2 carrier could further be used as a catalyst (Garcia-Segura et al., 2016; Su et al., 2011). From another perspective, Manenti et al. (2015) conducted solar photo-Fenton treatment of textile wastewater using different Fe^{3+}-organic ligand complexes, such as Fe^{3+}-oxalate and Fe^{3+}-citrate, which have high solubility and stability to prevent iron precipitation, and high photoactivity under UV-visible light. Among these, Fe^{3+}-oxalate achieved the best results because of its high quantum yield for Fe^{2+} production. The complex was formed in situ by adding $H_2C_2O_4 \cdot 2H_2O$ (an organic acid) and $FeCl_3$ to the wastewater.

Ganiyu et al. (2017) presented another application of iron-supporting materials, using them as functionalized cathodes in a heterogeneous electro-Fenton process, thereby preventing sludge production. The functionalized cathode acted both as an electrode and a catalyst source. In several cases, the catalysts are impregnated or supported on materials with a high capacity to generate H_2O_2, such as active carbon/fiber, carbon felt, graphite felt, and recently, carbon aerogel; the technique used influences the adhesion and mechanical wear of the catalyst from the cathode matrix (Ganiyu et al., 2018).

Table 3 presents the results of studies published over the past years focusing on heterogeneous Fenton treatment of real wastewater, highlighting the array of catalysts and techniques that have been analyzed and the discrepancy in the results, for different materials/technologies and raw wastewater characteristics.

6.3 Iron minerals and low-cost catalysts from waste

Several iron oxides may be used in their natural state in Fenton catalysis. Oxide hydroxides can be dehydroxylated to their oxides under specific conditions, with the ability to alter their size, orientation, dimensionality, and morphology (Wang et al., 2012). Of the 16 known iron oxides and hydroxides, some have been successfully used in heterogeneous catalysis, for example magnetite (Fe_3O_4), goethite (α-FeOOH), wüstite (FeO), maghemite (γ-Fe_2O_3), and hematite (α-Fe_2O_3) (Pouran et al., 2014; Wang et al., 2012). According to Pouran et al. (2014), magnetite, the most abundant Fe^{2+}-containing iron oxide, exhibits certain characteristics that distinguish it

from the other iron oxides, such as the presence of octahedral sites (significantly contributing to the catalytic effect) on its surface; magnetic properties, allowing easy separation from the reaction system; high dissolution rate and resultant electron mobility; and its spinel structure. Goethite is also highly suitable because of its ability to operate over a wide pH range, solar applications, high stability, environmental friendliness, and low price (Pouran et al., 2014).

The possibility of deriving Fenton catalysts from waste materials is an important development in this field, as low-cost catalysts could be produced under the circular economic concept. Sludge is the commonly utilized waste material that acts as a catalyst support, owing to its high carbon content. Gu et al. (2012) used simple physiochemical activation and carbonization processes to synthesize a porous carbon-containing magnetite from sewage sludge at a carbonization temperature of 600 °C. The catalyst was then analyzed for the degradation of the model compound 1-diazo-2-naphthol-4-sulfonic acid, achieving 96.6 % removal (90.2 % after three cycles), compared to 57.5 % obtained using commercial Fe_3O_4 nanoparticles. At high temperatures, the manufactured catalyst exhibited decreased activity owing to structural changes in the iron during thermal treatment. In another study (Grassi et al., 2020), a Fenton catalyst was obtained from the sludge of a water treatment plant after calcination at 600 °C, with hematite (Fe_2O_3) as the primary active phase (12.65 wt. % in calcined sludge). This waste-derived catalyst was used (0.75 $g \cdot L^{-1}$) in the Fenton degradation of amaranth dye, achieving 97 % decolorization after 30 min, at pH = 2.8, and 5.5 mM H_2O_2. The efficiency and stability of the catalyst were maintained after three cycles of reuse. Zhang et al. (2018) converted ferric and biological sludge from a real dyeing wastewater treatment plant into a magnetic biochar Fenton heterogeneous catalyst under hydrothermal conditions. 47 % COD and 49 % TOC removal were achieved after 30 min under optimized conditions (1 $g \cdot L^{-1}$ catalyst and 8.82 mM H_2O_2), and after four cycles; the leached iron was less than 0.9 $mg \cdot L^{-1}$ after five cycles.

Park et al. (2018) prepared a novel Fe-impregnated sugarcane residue biochar-based catalyst with one-step pyrolysis and used it as a Fenton catalyst to degrade the model compound, orange G. Under optimal conditions (22.1 mM H_2O_2, 0.5 $g \cdot L^{-1}$ catalyst with Fe content of 163.4 $mg \cdot g^{-1}$, and pH = 5.5), 99.7 % orange G removal was achieved (over 89 % after four cycles). Martins et al. (2012) analyzed the applicability of iron shavings as ZVI catalysts for the Fenton treatment of landfill leachate. After 60 min, 48 % COD removal was achieved for wastewater

pre-treated using biological methods, while 38 % COD removal was achieved for that pre-treated using biological and chemical methods. The iron shavings maintained a catalytic activity of over 60 % over four cycles. Martins et al. (2013) also used iron shavings without modification as Fenton catalysts, removing 60% TOC, 30 % COD, and 90 % phenol from olive mill wastewater after 30 min; however, the catalyst dosage was significantly high at 40 $g \cdot L^{-1}$ (with 35 mM H_2O_2 and pH 3).

Finally, Vilardi et al. (2018) reported 58.4 % COD removal from tannery wastewater using an iron-based coated olive stone as the heterogeneous Fenton catalyst. The olive stones were ground and coated, first with nano-ZVI (with $FeSO_4$ using the borohydride reduction method) and then with nano-magnetite (immersing the nano-ZVI-coated particles in a Fe^{2+}–Fe^{3+} solution), to obtain the catalyst. The reusability of the material was verified for up to five cycles after regeneration with NaOH and $C_2H_2O_4$ solutions.

6.4 Nanomaterials

Nanomaterials have a particularly high surface area, improving their suitability for wastewater treatment, namely as heterogeneous catalysts, owing to their low diffusion resistance, easy accessibility to reactants, and numerous active sites (Wang et al., 2012, 2016). The activity and selectivity of catalyst nanoparticles are highly dependent on their size, shape, and surface structure, as well as on their bulk and surface composition (Rosales et al., 2017). Nanoparticles can be commonly synthesized using several methods, such as chemical coprecipitation, hydrothermal treatment, and different physical-assisted methods, including the Langmuir-Blodgett technique, gamma-ray radiation, and microwave irradiation (Wang et al., 2016). Among iron oxides, nano-hematite is most widely prepared, because of its scientific and technological advantages as the most stable iron oxide under ambient conditions (Wang et al., 2012). Materials used for iron ion immobilization may also be analyzed for immobilizing nano-ZVI; however, the associated catalytic efficiency may decrease when immobilized onto support materials (Babuponnusami and Muthukumar, 2014; Wang et al., 2012).

Another notable application of nanoparticles as a heterogeneous Fenton catalyst was presented by Trotte et al. (2016), who synthesized iron nanoparticles by adding tea extracts of the yerba mate plant to a solution of $Fe(NO_3)_3$ and silica gel (acting as support). Under optimal conditions, 80% decolorization of the methyl orange solution was achieved; however, the authors could not

successfully recycle the catalyst, and the catalytic activity decreased to half in the second cycle. Carvalho and Carvalho (2017) also synthesized a Fenton nanocatalyst from tea extracts and $FeCl_3$ using SiO_2 as a support. The iron nanoparticles were immersed in the polyphenol compounds from the tea extract, which could sufficiently reduce Fe^{3+} to Fe^{2+} (but not to Fe^0), forming Fe^{2+}/Fe^{3+} oxide/hydroxide nanoparticles. The study achieved complete decolorization in less than 3 h under optimized conditions.

Nevertheless, the application of nanomaterials to wastewater treatment presents serious drawbacks. The primary concerns are separating them from the treated wastewater and their environmental toxicity (Poza-Nogueiras et al., 2018). Moreover, nanoparticles lose their reactivity due to coalescence into aggregates, reduction of specific area, poisoning of the active catalytic sites by adsorbed organic species, and the loss of supernatants during nanoparticle rinsing, which in turn hinders their reusability (Babuponnusami and Muthukumar, 2014; Poza-Nogueiras et al., 2018).The iron oxide surface may also require light for the Fe^{3+}-to-Fe^{2+} conversion (Wang et al., 2012).

These concerns hinder the wider application of nanomaterials in studies on real wastewater treatment, which therefore require extensive research before they can be implemented or even recognized at the industrial decision-making level. Therefore, further discussion of the results obtained with nanomaterials was not considered within the scope of this study.

Table 3. Compilation of results reported on the application of Fenton process with regeneration/reuse of the catalyst, and heterogeneous Fenton process, to real industrial wastewater treatment.

Operating conditions	Wastewater treated	Parameter	Removal (%)	Ref.	Notes
$[H_2O_2]$ = 29.41 mM; $[Fe^0]$ = 8.95 mM; pH = 3.0; t = 120 min; T = 24 ºC	Pulp bleaching wastewater	COD	58.4	Sevimli et al. (2014)	
$[H_2O_2]$ = 30 mM; Activated carbon-Fe(II) catalyst (7% wt. Fe) immobilized in a fixed bed; pH = 2.5; HRT = 22.5 min; T = 50 ºC	Textile (cotton dyeing) wastewater	TOC	73.6	Duarte et al. (2013)	H_2O_2 continuously fed (2 mL·min^{-1})
		COD	66.3		
		BOD_5	72.5		
		Color	92.7		
$[H_2O_2]$ = 2 mM; $[Fe^{2+}]$ = 0.36 mM; pH = 3.5; HRT = 60 min; T = ambient	Textile wastewater	TOC	83.0	Karthikeyan et al. (2011)	Followed by heterogeneous post-treatment in a fixed-bed reactor of activated carbon (from rice husk)
		COD	91.0		
		BOD_5	83.0		
		BOD_5/COD	0.21 to 0.39		
		SS	6.3		
		Aromatics	100		
$[H_2O_2]$ = 53 mM; $[Fe^{3+}$: oxalate catalyst] = 1.79:5.37 mM; pH = 2.8; t = 74 min; T = ambient; 20.2 kJ·L^{-1} solar irradiation	Textile wastewater	Color	100	Manenti et al. (2015)	Oxalate formed in-situ by addition of oxalic acid to the wastewater
		DOC	74.0		
$[H_2O_2]$ = 2.57 mM; [Fe/Sepiolite catalyst] = 0.5 g·L^{-1} (5% wt. Fe); pH = 3.0; t = 120 min; T = 30 ºC	Textile wastewater	TOC	25.0	Rodríguez et al. (2010)	
		COD	36.0		
		Color	35.0		
$[H_2O_2]$ = 83.84 mM; $[Fe^{2+}]$ = 6.11 mM; pH = 3.0; t = 10 min; T = ambient; 74.1 g·L^{-1} SiO_2	Textile wastewater	COD	86.7	Su et al. (2011)	Fluidized-bed Fenton, with Fe^{2+} supplied as Fe_2SO_4, and SiO_2 used as solid carrier
		Color	96.6		
$[H_2O_2]$ = 37.42 mM; [MICOS catalyst] = 4 g·L^{-1}; pH = 4.8; t = 120 min; T = 25 ºC	Tannery wastewater	COD	58.4	Vilardi et al. (2018)	MICOS obtained by soaking olive stones with Fe^{2+}/Fe^{3+} and ammonia
		Phenol	59.2		
$[H_2O_2]$ = 8.824 mM; [MBC catalyst] = 1 g·L^{-1}; pH = 3.0; t = 30 min; T = ambient	Textile wastewater	TOC	49.0	Zhang et al. (2018)	MBC obtained by hydrothermal carbonization from a 1:2 molar ratio of Fenton sludge:biological sludge
		COD	47.0		
		BOD_5/COD	0.26 to 0.68		
$[H_2O_2]$ = 175 mM; $[Fe^{2+}]$ = 6.123 mM; pH = 3.0; t = 24 h; T = 22 ºC	Municipal landfill leachate	COD	70.0	Bolobajev et al. (2014)	Fe^{2+} supplied from Fenton sludge; after 4 cycles, 60 % COD removal
		BOD_5/COD	20 % increase		
$[H_2O_2]$ = 394.1 mM; $[Fe^0]$ = 25 g·L^{-1} as iron shavings; pH = 2.0; t = 60 min; T = ambient	Landfill leachate	COD	48.0	Martins et al. (2012)	After biological (aerobic) treatment
		BOD_5/COD	0.04 to 0.27		
$[H_2O_2]$ = 1470 mM; $[Fe^0]$ = 358.1 mM; pH = 4.8; t = 24 h; T = ambient	Olive mill wastewater	COD	30.0	Kallel et al. (2009)	
$[H_2O_2]$ = 35 mM; $[Fe^0]$ = 40 g·L^{-1} as iron shavings; pH = 3.0; t = 30 min; T = ambient	Olive mill wastewater	TOC	60.0	Martins et al. (2013)	
		COD	30.0		
		Phenol	90.0		
$[H_2O_2]$ = 35 mM; $[Fe^0]$ = 12.3 g of iron shavings filling a 14.5 cm height tubular fixed bed reactor; pH = 3.0; 1 mL·min^{-1} flow; T = ambient	Olive mill wastewater	TOC	≈ 75.0	Martins et al. (2013)	Maximum removal achieved after 30 min, afterwards the column reactor clogs
		COD	33.3		
		Phenol	85.0		
$[H_2O_2]$ = 58.8 mM; $[Fe^0]$ = 35.81 mM; pH = 3.0; t = 90 min; T = ambient	Olive mill wastewater	COD	82.0	Ozdemir et al. (2010)	
		Phenol	63.4		
$[H_2O_2]$ = 735.3 mM; $[Fe^{2+}]$ = 0.895 mM; pH = 3.5; t = 60 min; T = ambient; IE with 40 g·L^{-1} Lewatit TP 207	Olive mill wastewater	COD	81.0	Reis et al. (2018)	Fe^{2+} supplied as Fe_2SO_4, with 90 % recovery of reusable catalyst after treatment by IE
		BOD_5	75.0		
		BOD_5/COD	0.38 to 0.50		
		Phenol	97.0		
$[H_2O_2]$ = 10 mM; $[Fe^{2+}]$ = 1 mM; pH = 3.0; t = 200 min; T = 20 ºC	Fine chemical wastewater	COD	59.0	Cao et al. (2009)	Fe^{2+} supplied from Fenton sludge; after 6 cycles, 64.6 % COD removal
		BOD_5/COD	0.06 to 0.38		
$[H_2O_2]$ = 59.29 mM; $[Fe^{2+}]$ = 6.446 mM; pH = 3.0; t = 24 h; T = 22 ºC	Semicoke landfill leachate	COD	65.0	Bolobajev et al. (2014)	Fe^{2+} supplied from Fenton sludge; after 4 cycles, 60 % COD removal
		BOD_5/COD	20 % increase		
$[H_2O_2]$ = 317.7 mM; [Fe_2O_3/SBA-15 catalyst] = 2.9 g (19 % wt. Fe) packed bed in a 15 cm height tubular fixed bed reactor; pH = 3.0; 0.25 mL·min^{-1} flow; HRT = 3.8 min; T = 80 ºC	Pharmaceutical wastewater	TOC	59.0	Melero et al. (2009)	
		COD	81.0		
		BOD_5	71.0		
		BOD_5/COD	0.20 to 0.30		
$[H_2O_2]$ = 13.53 mM; $[Fe^0]$ = 1.2 g·L^{-1} as commercial iron powder; pH = 3.0; t = 60 min; T = 22 ºC	Pharmaceutical wastewater	TOC	64.0	Segura et al. (2013)	Aeration at 5 L·min^{-1}
$[H_2O_2]$ = 13.53 mM; $[Fe^0]$ = 1.2 g·L^{-1} as iron shavings; pH = 3.0; t = 60 min; T = 22 ºC	Pharmaceutical wastewater	TOC	75.0	Segura et al. (2013)	Aeration at 5 L·min^{-1}
$[H_2O_2]$ = 90.62 mM; $[Fe^{2+}]$ = 7.073 mM; pH = 3.0; t = 24 h; T = 22 ºC	Plywood manufacturing (wood soaking) wastewater	COD	80.0	Bolobajev et al. (2014)	After $(Fe_2SO_4)_3$ coagulation; Fe^{2+} supplied from Fenton sludge; after 4 cycles, 70 % COD removal

7. Future prospects and challenges

The increasing industrial pollution and environmental health concerns, and resultant increase in legal measures, have renewed the interest in AOPs for wastewater treatment over the past years. However, the primary focus is no longer on the basic principles of such methods or optimizing the operating conditions. It has recently been laid on discovering novel methods to conduct the well-known treatment processes, such as the conventional homogeneous Fenton process, to meet environmental (legal) standards, with operating costs that do not hinder their full-scale application in industries. During the last decade, efforts have been made to find/synthesize materials as alternatives to conventional iron salt Fenton catalysts and/or regenerate and reuse the catalyst, in contrast to optimizing the application of existing materials. This trend is expected to continue, with further advancements for full-scale implementation. Other studies will possibly be published in the future on applying the Fenton process using new types of nanomaterials, new solid matrices impregnated with iron solution, reusing iron wastes from different industrial sectors, etc. The aim should be to produce reusable materials, avoiding the continuous extraction of iron ore and its subsequent discharge after (single) use, transitioning from a linear to a circular economy. Sustainable catalyst should have properties, such as low leaching rate, high stability over a wide pH range, high catalytic activity, and low manufacturing costs. Lifecycle analysis may be a suitable tool to facilitate the search for viable materials and techniques for developing new catalysts. Comninellis et al. (2008) stated that, “the treatment of wastewaters that have been generated without the application of ‘cleaner production’ and ‘waste minimization’ principles is a losing game, ultimately costing all parties materials and energy resources”. In the future, research should also be conducted on analyzing and improving the lifecycle of the heterogeneous catalyst, such as determining the predominant pathway between heterogeneous and homogeneous catalysis to pollutant degradation depending on the operating conditions.

However, these future prospects must take into account that many challenges yet remain unanswered in this field, which should receive further attention in future studies. One of them is a lack of studies on the heterogeneous Fenton process for real wastewater, which needs to be addressed before pilot plant or full-scale studies can be conducted. As the wastewater

characteristics influence the performance of the Fenton process, the most suitable technique cannot be generalized for any particular type of wastewater. Finally, each industry should optimize not only the performance but also the economic and environmental factors, as well as intrinsic factors, such as wastewater flowrate.

Evaluating the operating cost associated with novel technical solutions is often overlooked in the literature, which prevents a higher impact in influencing decision-making. In particular, full pilot plant and real-scale economic analysis of the proposed processes is yet lacking. A complete economic analysis should include equipment and implementation expenses, amortization, reagent demand, energy costs, and sludge disposal (Ochando-Pulido et al., 2017). Moreover, the Fenton processes should be further developed to use these methods at full-scale. For example, several studies have reported an increase in wastewater biodegradability after Fenton processes (Pintor et al., 2011; Reis et al., 2018; Zhang et al., 2018), which indicates that it could be economically efficient as a pre-treatment method followed by a conventional biological treatment. However, intermediate compounds formed during the Fenton reaction are sometimes more toxic than the original compounds present in wastewater. One of the primary challenges in this field is to determine the best layout for incorporating the Fenton processes in full-scale treatment plants, namely before or after biological treatment, or between two stages of biological treatment. In fact, most AOP toxicity studies applied standard ecotoxicity test methods, and did not study real bacterial populations from industrial biological reactors (Esteves et al., 2016; Martins et al., 2013), which highlights the lack of necessary information for full-scale application of Fenton processes.

Another significant issue is the need to remove the microcontaminants, including AOX or phenol derivatives, that are often more toxic and environmentally hazardous than the commonly studied parameters, such as COD or TOC. Within all the studies compiled in this review, only nine have been on phenolic compounds and four on AOX. Due the environmental impact of these groups of compounds, further studies to control their emissions should be urgently conducted.

8. Conclusions and final remarks

The popularity of Fenton processes in wastewater treatment has been due to its simple operation and established advantages. However, in case of real wastewaters which are produced at flowrates ranging thousands of cubic meters per day, the continuous wastage of chemicals, particularly iron catalysts, and the associated iron sludge production/management strongly hinders full-scale application.

This review highlighted the shift in attention since the last decade from the homogeneous Fenton process and its developed variations to emerging technologies, including catalyst regeneration and replacement by heterogeneous matrices. Therefore, several studies have been published on the synthesis of new catalysts to substitute iron salt for achieving a green, sustainable method of conducting the Fenton process. By summarizing the key results obtained over the last few years, this review shows that production of effective catalysts is in its initial stage; studies have primarily been conducted at the lab scale with degradation of synthetic target solutions, implying that more time will be required to achieve full-scale implementation of such techniques. However, this study sheds light on the course of innovations and the current research scenario in this field and presents several promising perspectives on full-scale application of Fenton processes to industrial wastewater treatment.

Acknowledgements

Thanks are due to FCT/MCTES for the financial support to CESAM (UIDP/50017/2020 + UIDB/50017/2020), through national funds. J. P. Ribeiro acknowledges FCT – Fundação para a Ciência e a Tecnologia, I.P. for his PhD Grant (SFRH/BD/141133/2018).

References

Adityosulindro, S., Barthe, L., González-Labrada, K., Jáuregui Haza, U.J., Delmas, H., Julcour, C., 2017. Sonolysis and sono-Fenton oxidation for removal of ibuprofen in (waste)water. Ultrason. Sonochem. 39, 889–896. https://doi.org/10.1016/j.ultsonch.2017.06.008

Ahile, U.J., Wuana, R.A., Itodo, A.U., Sha'Ato, R., Dantas, R.F., 2020. A review on the use of chelating agents as an alternative to promote photo-Fenton at neutral pH: Current trends, knowledge gap and future studies. Sci. Total Environ. 710, 134872. https://doi.org/10.1016/j.scitotenv.2019.134872

Aleksic, M., Kusic, H., Koprivanac, N., Leszczynska, D., Bozic, A.L., 2010. Heterogeneous Fenton type processes for the degradation of organic dye pollutant in water - The application of zeolite assisted AOPs. Desalination 257, 22–29. https://doi.org/10.1016/j.desal.2010.03.016

Altin, A., Altin, S., Yildirim, O., 2017. Treatment of kraft pulp and paper mill wastewater by electro-fenton/electro-coagulation process. J. Environ. Prot. Ecol. 18, 652–661.

Ashrafi, O., Yerushalmi, L., Haghighat, F., 2015. Wastewater treatment in the pulp-and-paper industry: A review of treatment processes and the associated greenhouse gas emission. J. Environ. Manage. 158, 146–157. https://doi.org/10.1016/j.jenvman.2015.05.010

Atmaca, E., 2009. Treatment of landfill leachate by using electro-Fenton method. J. Hazard. Mater. 163, 109–114. https://doi.org/10.1016/j.jhazmat.2008.06.067

Babuponnusami, A., Muthukumar, K., 2014. A review on Fenton and improvements to the Fenton process for wastewater treatment. J. Environ. Chem. Eng. 2, 557–572. https://doi.org/10.1016/j.jece.2013.10.011

Bae, W., Won, H., Hwang, B., de Toledo, R.A., Chung, J., Kwon, K., Shim, H., 2015. Characterization of refractory matters in dyeing wastewater during a full-scale Fenton process following pure-oxygen activated sludge treatment. J. Hazard. Mater. 287, 421–428. https://doi.org/10.1016/j.jhazmat.2015.01.052

Balabanič, D., Hermosilla, D., Merayo, N., Klemenčič, A.K., Blanco, A., 2012. Comparison of different wastewater treatments for removal of selected endocrine-disruptors from paper mill wastewaters. J. Environ. Sci. Heal. Part A Toxic/hazardous Subst. Environ. Eng. 47, 1350–1363. https://doi.org/10.1080/10934529.2012.672301

Bautista, P., Mohedano, A.F., Casas, J.A., Zazo, J.., Rodríguez, J.., 2008. An overview of the application of Fenton oxidation to industrial wastewaters treatment. J. Chem. Technol. Biotechnol. 83, 1323–1338. https://doi.org/10.1002/jctb

Bautista, P., Mohedano, A.F., Gilarranz, M.A., Casas, J.A., Rodriguez, J.J., 2007. Application of Fenton oxidation to cosmetic wastewaters treatment. J. Hazard. Mater. 143, 128–134. https://doi.org/10.1016/j.jhazmat.2006.09.004

Belalcázar-Saldarriaga, A., Prato-Garcia, D., Vasquez-Medrano, R., 2018. Photo-Fenton processes in raceway reactors: Technical, economic, and environmental implications

during treatment of colored wastewaters. J. Clean. Prod. 182, 818–829. https://doi.org/10.1016/j.jclepro.2018.02.058

Bensalah, N., Bedoui, A., Chellam, S., Abdel-Wahab, A., 2013. Electro-Fenton Treatment of Photographic Processing Wastewater. Clean - Soil, Air, Water 41, 635–644. https://doi.org/10.1002/clen.201200521

Bianco, B., De Michelis, I., Vegliò, F., 2011. Fenton treatment of complex industrial wastewater: Optimization of process conditions by surface response method. J. Hazard. Mater. 186, 1733–1738. https://doi.org/10.1016/j.jhazmat.2010.12.054

Blanco, J., Torrades, F., De la Varga, M., García-Montaño, J., 2012. Fenton and biological-Fenton coupled processes for textile wastewater treatment and reuse. Desalination 286, 394–399. https://doi.org/10.1016/j.desal.2011.11.055

Bokare, A.D., Choi, W., 2014. Review of iron-free Fenton-like systems for activating H2O2 in advanced oxidation processes. J. Hazard. Mater. 275, 121–135.

Bokare, A.D., Choi, W., 2009. Zero-Valent Aluminum for Oxidative Degradation of Aqueous Organic Pollutants. Environ. Sci. Technol. 43, 7130–7135.

Bolobajev, J., Kattel, E., Viisimaa, M., Goi, A., Trapido, M., Tenno, T., Dulova, N., 2014. Reuse of ferric sludge as an iron source for the Fenton-based process in wastewater treatment. Chem. Eng. J. 255, 8–13. https://doi.org/10.1016/j.cej.2014.06.018

Brink, A., Sheridan, C.M., Harding, K.G., 2017. The Fenton oxidation of biologically treated paper and pulp mill effluents: A performance and kinetic study. Process Saf. Environ. Prot. 107, 206–215. https://doi.org/10.1016/j.psep.2017.02.011

Cañizares, P., Paz, R., Sáez, C., Rodrigo, M.A., 2009. Costs of the electrochemical oxidation of wastewaters: A comparison with ozonation and Fenton oxidation processes. J. Environ. Manage. 90, 410–420. https://doi.org/10.1016/j.jenvman.2007.10.010

Cao, G., Sheng, M., Niu, W., Fei, Y., Li, D., 2009. Regeneration and reuse of iron catalyst for Fenton-like reactions. J. Hazard. Mater. 172, 1446–1449. https://doi.org/10.1016/j.jhazmat.2009.08.010

Carvalho, S.S.F., Carvalho, N.M.F., 2017. Dye degradation by green heterogeneous Fenton catalysts prepared in presence of Camellia sinensis. J. Environ. Manage. 187, 82–88. https://doi.org/10.1016/j.jenvman.2016.11.032

Casado, J., 2019. Towards industrial implementation of Electro-Fenton and derived technologies for wastewater treatment: A review. J. Environ. Chem. Eng. 7. https://doi.org/10.1016/j.jece.2018.102823

Chagas, P.M., Caetano, A.A., Tireli, A.A., Cesar, P.H., Corrêa, A.D., Guimarães, I. do R., 2019. Use of an Environmental Pollutant From Hexavalent Chromium Removal as a Green Catalyst in The Fenton Process. Nat. Res. - Sci. Reports 9, 1–15. https://doi.org/10.1038/s41598-019-49196-9

Comninellis, C., Kapalka, A., Malato, S., Parsons, S.A., Poulios, I., Mantzavinos, D., 2008. Advanced oxidation processes for water treatment: advances and trends for R&D. J. Chem. Technol. Biotechnol. 83, 769–776. https://doi.org/10.1002/jctb.1873

De Luca, A., Dantas, R.F., Esplugas, S., 2014. Assessment of iron chelates efficiency for photo-Fenton at neutral pH. Water Res. 61, 232–242. https://doi.org/10.1016/j.watres.2014.05.033

Dewil, R., Mantzavinos, D., Poulios, I., Rodrigo, M.A., 2017. New perspectives for Advanced Oxidation Processes. J. Environ. Manage. 195, 93–99. https://doi.org/10.1016/j.jenvman.2017.04.010

Duarte, F., Morais, V., Maldonado-Hódar, F.J., Madeira, L.M., 2013. Treatment of textile effluents by the heterogeneous Fenton process in a continuous packed-bed reactor using Fe/activated carbon as catalyst. Chem. Eng. J. 232, 34–41. https://doi.org/10.1016/j.cej.2013.07.061

Dulova, N., Trapido, M., Dulov, A., 2011. Catalytic degradation of picric acid by heterogeneous Fenton - based processes. Environ. Technol. 32, 439–446. https://doi.org/10.1080/09593330.2010.501823

Durán, A., Monteagudo, J.M., San Martín, I., 2012. Photocatalytic treatment of an industrial effluent using artificial and solar UV radiation: An operational cost study on a pilot plant scale. J. Environ. Manage. 98, 1–4. https://doi.org/10.1016/j.jenvman.2011.12.007

Eskelinen, K., Särkkä, H., Kurniawan, T.A., Sillanpää, M.E.T., 2010. Removal of recalcitrant contaminants from bleaching effluents in pulp and paper mills using ultrasonic irradiation and Fenton-like oxidation, electrochemical treatment, and/or chemical precipitation: A comparative study. Desalination 255, 179–187. https://doi.org/10.1016/j.desal.2009.12.024

Esteves, B.M., Rodrigues, C.S.D., Boaventura, R.A.R., Maldonado-Hódar, F.J., Madeira, L.M., 2016. Coupling of acrylic dyeing wastewater treatment by heterogeneous Fenton oxidation in a continuous stirred tank reactor with biological degradation in a sequential batch reactor. J. Environ. Manage. 166, 193–203. https://doi.org/10.1016/j.jenvman.2015.10.008

Fayazi, M., Taher, M.A., Afzali, D., Mostafavi, A., 2016. Enhanced Fenton-like degradation of methylene blue by magnetically activated carbon/hydrogen peroxide with hydroxylamine as Fenton enhancer. J. Mol. Liq. 216, 781–787. https://doi.org/10.1016/j.molliq.2016.01.093

Feng, F., Xu, Z., Li, X., You, W., Zhen, Y., 2010. Advanced treatment of dyeing wastewater towards reuse by the combined Fenton oxidation and membrane bioreactor process. J. Environ. Sci. 22, 1657–1665. https://doi.org/10.1016/S1001-0742(09)60303-X

Fernandes, L., Lucas, M.S., Maldonado, M.I., Oller, I., Sampaio, A., 2014. Treatment of pulp mill wastewater by Cryptococcus podzolicus and solar photo-Fenton: A case study. Chem. Eng. J. 245, 158–165. https://doi.org/10.1016/j.cej.2014.02.043

Ganiyu, S.O., Huong Le, T.X., Bechelany, M., Esposito, G., Van Hullebusch, E.D., Oturan, M.A., Cretin, M., 2017. A hierarchical CoFe-layered double hydroxide modified carbon-felt cathode for heterogeneous electro-Fenton process. J. Mater. Chem. A 5, 3655–3666. https://doi.org/10.1039/c6ta09100h

Ganiyu, S.O., Zhou, M., Martínez-Huitle, C.A., 2018. Heterogeneous electro-Fenton and photoelectro-Fenton processes: A critical review of fundamental principles and application for water/wastewater treatment. Appl. Catal. B Enviromental 235, 103–129. https://doi.org/10.1016/j.apcatb.2018.04.044

Gao, Y., Wang, Y., Zhang, H., 2015. Removal of Rhodamine B with Fe-supported bentonite as heterogeneous photo-Fenton catalyst under visible irradiation. Appl. Catal. B Enviromental 178, 29–36. https://doi.org/10.1016/j.apcatb.2014.11.005

Garcia-Segura, S., Bellotindos, L.M., Huang, Y.-H., Brillas, E., Lu, M.-C., 2016. Fluidized-bed Fenton process as alternative wastewater treatment technology - A review. J. Taiwan Inst. Chem. Eng. 67, 211–225. https://doi.org/10.1016/j.jtice.2016.07.021

Gernjak, W., Maldonado, M.I., Malato, S., Cáceres, J., Krutzler, T., Glaser, A., Bauer, R., 2004. Pilot-plant treatment of olive mill wastewater (OMW) by solar TiO2 photocatalysis and

solar photo-Fenton. Sol. Energy 77, 567–572. https://doi.org/10.1016/j.solener.2004.03.030

Ghanbari, F., Moradi, M., 2015. A comparative study of electrocoagulation, electrochemical Fenton, electro-Fenton and peroxi-coagulation for decolorization of real textile wastewater: Electrical energy consumption and biodegradability improvement. J. Environ. Chem. Eng. 3, 499–506. https://doi.org/10.1016/j.jece.2014.12.018

Grassi, P., Drumm, F.C., Georgin, J., Franco, D.S.P., Foletto, E.L., Dotto, G.L., Jahn, S.L., 2020. Water treatment plant sludge as iron source to catalyze a heterogeneous photo-Fenton reaction. Environ. Technol. Innov. 17, 100544. https://doi.org/10.1016/j.eti.2019.100544

Gu, L., Zhu, N., Zhou, P., 2012. Preparation of sludge derived magnetic porous carbon and their application in Fenton-like degradation of 1-diazo-2-naphthol-4-sulfonic acid. Bioresour. Technol. 118, 638–642. https://doi.org/10.1016/j.biortech.2012.05.102

Gümüş, D., Akbal, F., 2016. Comparison of Fenton and electro-Fenton processes for oxidation of phenol. Process Saf. Environ. Prot. 103, 252–258. https://doi.org/10.1016/j.psep.2016.07.008

Güneş, E., Demir, E., Güneş, Y., Hanedar, A., 2019. Characterization and treatment alternatives of industrial container and drum cleaning wastewater: Comparison of Fenton-like process and combined coagulation/oxidation processes. Sep. Purif. Technol. 209, 426–433. https://doi.org/10.1016/j.seppur.2018.07.060

Guo, S., Zhang, G., Wang, J., 2014. Photo-Fenton degradation of rhodamine B using Fe2O3-Kaolin as heterogeneous catalyst: Characterization , process optimization and mechanism. J. Colloid Interface Sci. 433, 1–8. https://doi.org/10.1016/j.jcis.2014.07.017

Guo, Y., Xue, Q., Zhang, H., Wang, N., Chang, S., Wang, H., Pang, H., Chen, H., 2018. Treatment of real benzene dye intermediates wastewater by the Fenton method: Characteristics and multi-response optimization. RSC Adv. 8, 80–90. https://doi.org/10.1039/c7ra09404c

Hasan, D.B., Abdul Aziz, A.R., Daud, W.M.A.W., 2012. Oxidative mineralisation of petroleum refinery effluent using Fenton-like process. Chem. Eng. Res. Des. 90, 298–307. https://doi.org/10.1016/j.cherd.2011.06.010

He, D.-Q., Zhang, Y.-J., Pei, D.-N., Huang, G.-X., Liu, C., Li, J., Yu, H.-Q., 2020. Degradation of benzoic acid in an advanced oxidation process: The effects of reducing agents. J. Hazard. Mater. 382. https://doi.org/10.1016/j.jhazmat.2019.121090

He, H., Zhou, Z., 2017. Electro-fenton process for water and wastewater treatment. Crit. Rev. Environ. Sci. Technol. 47, 2100–2131. https://doi.org/10.1080/10643389.2017.1405673

Hermosilla, D., Cortijo, M., Huang, C.P., 2009. Optimizing the treatment of landfill leachate by conventional Fenton and photo-Fenton processes. Sci. Total Environ. 407, 3473–3481. https://doi.org/10.1016/j.scitotenv.2009.02.009

Hermosilla, D., Merayo, N., Gascó, A., Blanco, Á., 2015. The application of advanced oxidation technologies to the treatment of effluents from the pulp and paper industry: A review. Environ. Sci. Pollut. Res. 22, 168–191. https://doi.org/10.1007/s11356-014-3516-1

Hermosilla, D., Merayo, N., Ordóñez, R., Blanco, ángeles, 2012. Optimization of conventional Fenton and ultraviolet-assisted oxidation processes for the treatment of reverse osmosis retentate from a paper mill. Waste Manag. 32, 1236–1243. https://doi.org/10.1016/j.wasman.2011.12.011

Hodaifa, G., Ochando-Pulido, J.M., Rodriguez-Vives, S., Martinez-Ferez, A., 2013. Optimization of continuous reactor at pilot scale for olive-oil mill wastewater treatment by Fenton-like process. Chem. Eng. J. 220, 117–124. https://doi.org/10.1016/j.cej.2013.01.065

Hubbe, M.A., Metts, J.R., Hermosilla, D., Blanco, M.A., Yerushalmi, L., Haghighat, F., Lindholm-Lehto, P., Khodaparast, Z., Kamali, M., Elliott, A., 2016. Wastewater Treatment and Reclamation: A Review of Pulp and Paper Industry Practices and Opportunities. BioResources 11, 7953–8091. https://doi.org/10.15376/biores.11.3.hubbe

Kakavandi, B., Ahmadi, M., 2019. Efficient treatment of saline recalcitrant petrochemical wastewater using heterogeneous UV-assisted sono-Fenton process. Ultrason. Sonochem. 56, 25–36. https://doi.org/10.1016/j.ultsonch.2019.03.005

Kallel, M., Belaid, C., Boussahel, R., Ksibi, M., Montiel, A., Elleuch, B., 2009. Olive mill wastewater degradation by Fenton oxidation with zero-valent iron and hydrogen peroxide. J. Hazard. Mater. 163, 550–554. https://doi.org/10.1016/j.jhazmat.2008.07.006

Kamali, M., Khodaparast, Z., 2015. Review on recent developments on pulp and paper mill wastewater treatment. Ecotoxicol. Environ. Saf. 114, 326–342.

https://doi.org/10.1016/j.ecoenv.2014.05.005

Karthikeyan, S., Titus, A., Gnanamani, A., Mandal, A.B., Sekaran, G., 2011. Treatment of textile wastewater by homogeneous and heterogeneous Fenton oxidation processes. Desalination 281, 438–445. https://doi.org/10.1016/j.desal.2011.08.019

Kishimoto, N., Kitamura, T., Kato, M., Otsu, H., 2013. Reusability of iron sludge as an iron source for the electrochemical Fenton-type process using Fe2+/HOCl system. Water Res. 47, 1919–1927. https://doi.org/10.1016/j.watres.2013.01.021

Klidi, N., Proietto, F., Vicari, F., Galia, A., Ammar, S., Gadri, A., Scialdone, O., 2019. Electrochemical treatment of paper mill wastewater by electro-Fenton process. J. Electroanal. Chem. 841, 166–171. https://doi.org/10.1016/j.jelechem.2019.04.022

Lal, K., Garg, A., 2017. Utilization of dissolved iron as catalyst during Fenton-like oxidation of pretreated pulping effluent. Process Saf. Environ. Prot. 111, 766–774. https://doi.org/10.1016/j.psep.2017.09.005

Lan, H., Wang, A., Liu, R., Liu, H., Qu, J., 2015. Heterogeneous photo-Fenton degradation of acid red B over Fe2O3 supported on activated carbon fiber. J. Hazard. Mater. 285, 167–172.

Lucas, M.S., Peres, J.A., 2009. Removal of COD from olive mill wastewater by Fenton's reagent: Kinetic study. J. Hazard. Mater. 168, 1253–1259. https://doi.org/10.1016/j.jhazmat.2009.03.002

Lucas, M.S., Peres, J.A., Amor, C., Prieto-Rodríguez, L., Maldonado, M.I., Malato, S., 2012. Tertiary treatment of pulp mill wastewater by solar photo-Fenton. J. Hazard. Mater. 225–226, 173–181. https://doi.org/10.1016/j.jhazmat.2012.05.013

Mandal, T., Maity, S., Dasgupta, D., Datta, S., 2010. Advanced oxidation process and biotreatment: Their roles in combined industrial wastewater treatment. Desalination 250, 87–94. https://doi.org/10.1016/j.desal.2009.04.012

Manenti, D.R., Soares, P.A., Módenes, A.N., Espinoza-Quiñones, F.R., Boaventura, R.A.R., Bergamasco, R., Vilar, V.J.P., 2015. Insights into solar photo-Fenton process using iron(III)-organic ligand complexes applied to real textile wastewater treatment. Chem. Eng. J. 266, 203–212. https://doi.org/10.1016/j.cej.2014.12.077

Martins, P.J.M., Reis, P.M., Martins, R.C., Gando-Ferreira, L.M., Quinta-Ferreira, R.M., 2017.

Iron recovery from the Fenton's treatment of winery effluent using an ion-exchange resin. J. Mol. Liq. 242, 505–511. https://doi.org/10.1016/j.molliq.2017.07.041

Martins, R.C., Henriques, L.R., Quinta-Ferreira, R.M., 2013. Catalytic activity of low cost materials for pollutants abatement by Fenton's process. Chem. Eng. Sci. 100, 225–233. https://doi.org/10.1016/j.ces.2013.03.024

Martins, R.C., Lopes, D. V., Quina, M.J., Quinta-Ferreira, R.M., 2012. Treatment improvement of urban landfill leachates by Fenton-like process using ZVI. Chem. Eng. J. 192, 219–225. https://doi.org/10.1016/j.cej.2012.03.053

Melero, J.A., Martínez, F., Botas, J.A., Molina, R., Pariente, M.I., 2009. Heterogeneous catalytic wet peroxide oxidation systems for the treatment of an industrial pharmaceutical wastewater. Water Res. 43, 4010–4018. https://doi.org/10.1016/j.watres.2009.04.012

Miklos, D.B., Remy, C., Jekel, M., Linden, K.G., Drewes, J.E., Hübner, U., 2018. Evaluation of advanced oxidation processes for water and wastewater treatment - A critical review. Water Res. 139, 118–131. https://doi.org/10.1016/j.watres.2018.03.042

Mohajeri, S., Aziz, H.A., Isa, M.H., Zahed, M.A., Adlan, M.N., 2010. Statistical optimization of process parameters for landfill leachate treatment using electro-Fenton technique. J. Hazard. Mater. 176, 749–758. https://doi.org/10.1016/j.jhazmat.2009.11.099

Moreira, F.C., Boaventura, R.A.R., Brillas, E., Vilar, V.J.P., 2017. Electrochemical advanced oxidation processes: A review on their application to synthetic and real wastewaters. Appl. Catal. B Environ. 202, 217–261. https://doi.org/10.1016/j.apcatb.2016.08.037

Moussavi, G., Aghanejad, M., 2014. The performance of electrochemical peroxidation process for COD reduction and biodegradability improvement of the wastewater from a paper recycling plant. Sep. Purif. Technol. 132, 182–186. https://doi.org/10.1016/j.seppur.2014.05.007

Munoz, M., Pliego, G., Pedro, Z.M., Casas, J.A., Rodriguez, J.J., 2014. Application of intensified Fenton oxidation to the treatment of sawmill wastewater. Chemosphere 109, 34–41. https://doi.org/10.1016/j.chemosphere.2014.02.062

Nidheesh, P. V., Gandhimathi, R., 2012. Trends in electro-Fenton process for water and wastewater treatment: An overview. Desalination 299, 1–15. https://doi.org/10.1016/j.desal.2012.05.011

Nidheesh, P. V., Zhou, M., Oturan, M.A., 2018. An overview on the removal of synthetic dyes from water by electrochemical advanced oxidation processes. Chemosphere 197, 210–227. https://doi.org/10.1016/j.chemosphere.2017.12.195

Ochando-Pulido, J.M., Pimentel-Moral, S., Verardo, V., Martinez-Ferez, A., 2017. A focus on advanced physico-chemical processes for olive mill wastewater treatment. Sep. Purif. Technol. 179, 161–174. https://doi.org/10.1016/j.seppur.2017.02.004

Oller, I., Malato, S., Sánchez-Pérez, J.A., 2011. Combination of Advanced Oxidation Processes and biological treatments for wastewater decontamination - A review. Sci. Total Environ. 409, 4141–4166. https://doi.org/10.1016/j.scitotenv.2010.08.061

Özdemir, C., Tezcan, H., Sahinkaya, S., Kalipci, E., 2010. Pretreatment of Olive Oil Mill Wastewater by Two Different Applications of Fenton Oxidation Processes. Clean - Soil, Air, Water 38, 1152–1158. https://doi.org/10.1002/clen.201000222

Padoley, K. V., Mudliar, S.N., Banerjee, S.K., Deshmukh, S.C., Pandey, R.A., 2011. Fenton oxidation: A pretreatment option for improved biological treatment of pyridine and 3-cyanopyridine plant wastewater. Chem. Eng. J. 166, 1–9. https://doi.org/10.1016/j.cej.2010.06.041

Park, J.-H., Wang, J.J., Xiao, R., Tafti, N., DeLaune, R.D., Seo, D.-C., 2018. Degradation of Orange G by Fenton-like reaction with Fe-impregnated biochar catalyst. Bioresour. Technol. 249, 368–376. https://doi.org/10.1016/j.biortech.2017.10.030

Pintor, A.M.A., Vilar, V.J.P., Boaventura, R.A.R., 2011. Decontamination of cork wastewaters by solar-photo-Fenton process using cork bleaching wastewater as H2O2 source. Sol. Energy 85, 579–587. https://doi.org/10.1016/j.solener.2011.01.003

Pliego, G., Zazo, J.A., Blasco, S., Casas, J.A., Rodriguez, J.J., 2012. Treatment of highly polluted hazardous industrial wastewaters by combined coagulation - Adsorption and high-temperature Fenton oxidation. Ind. Eng. Chem. Res. 51, 2888–2896. https://doi.org/10.1021/ie202587b

Pliego, G., Zazo, J.A., Casas, J.A., Rodriguez, J.J., 2013. Case study of the application of Fenton process to highly polluted wastewater from power plant. J. Hazard. Mater. 252–253, 180–185. https://doi.org/10.1016/j.jhazmat.2013.02.042

Pouran, S.R., Raman, A.A.A., Daud, W.M.A.W., 2014. Review on the application of modified

iron oxides as heterogeneous catalysts in Fenton reactions. J. Clean. Prod. 64, 24–35. https://doi.org/10.1016/j.jclepro.2013.09.013

Poyatos, J.M., Muñio, M.M., Almecija, M.C., Torres, J.C., Hontoria, E., Osorio, F., 2010. Advanced oxidation processes for wastewater treatment: State of the art. Water. Air. Soil Pollut. 205, 187–204. https://doi.org/10.1007/s11270-009-0065-1

Poza-Nogueiras, V., Rosales, E., Pazos, M., Sanromán, M.Á., 2018. Current advances and trends in electro-Fenton process using heterogeneous catalysts - A review. Chemosphere 201, 399–416. https://doi.org/10.1016/j.chemosphere.2018.03.002

Queirós, S., Morais, V., Rodrigues, C.S.D., Maldonado-Hódar, F.J., Madeira, L.M., 2015. Heterogeneous Fenton's oxidation using Fe/ZSM-5 as catalyst in a continuous stirred tank reactor. Sep. Purif. Technol. 141, 235–245. https://doi.org/10.1016/j.seppur.2014.11.046

Rabelo, M.D., Bellato, C.R., Silva, C.M., Ruy, R.B., Silva, C.A.B. da, Nunes, W.G., 2014. Application of Photo-Fenton Process for the Treatment of Kraft Pulp Mill Effluent. Adv. Chem. Eng. Sci. 04, 483–490. https://doi.org/10.4236/aces.2014.44050

Rahmani, A.R., Mousavi-Tashar, A., Masoumi, Z., Azarian, G., 2019. Integrated advanced oxidation process, sono-Fenton treatment, for mineralization and volume reduction of activated sludge. Ecotoxicol. Environ. Saf. 168, 120–126. https://doi.org/10.1016/j.ecoenv.2018.10.069

Ramos, J.M.P., Pereira-Queiroz, N.M., Santos, D.H.S., Nascimento, J.R., Carvalho, C.M. de, Tonholo, J., Zanta, C.L.P.S., 2019. Printing ink effluent remediation: A comparison between electrochemical and Fenton treatments. J. Water Process Eng. 31, 100803. https://doi.org/10.1016/j.jwpe.2019.100803

Ramos, P.B., Vitale, P., Barreto, G.P., Aparicio, F., Dublan, M. de los Á., Eyler, G.N., 2020. Treatment of real non-biodegradable wastewater: Feasibility analysis of a zero-valent iron/H2O2 process. J. Environ. Chem. Eng. 8, 103954. https://doi.org/10.1016/j.jece.2020.103954

Reis, P.M., Martins, P.J.M., Martins, R.C., Gando-Ferreira, L.M., Quinta-Ferreira, R.M., 2018. Integrating Fenton's process and ion exchange for olive mill wastewater treatment and iron recovery. Environ. Technol. (United Kingdom) 39, 308–316. https://doi.org/10.1080/09593330.2017.1299797

Ribeiro, J.P., Marques, C.C., Portugal, I., Nunes, M.I., 2020a. AOX removal from pulp and paper wastewater by Fenton and photo-Fenton processes: A real case-study. Energy Reports 6, 770–775. https://doi.org/10.1016/j.egyr.2019.09.068

Ribeiro, J.P., Marques, C.C., Portugal, I., Nunes, M.I., 2020b. Fenton processes for AOX removal from a kraft pulp bleaching industrial wastewater: Optimisation of operating conditions and cost assessment. J. Environ. Chem. Eng. 8, 104032. https://doi.org/10.1016/j.jece.2020.104032

Rodríguez, A., Ovejero, G., Sotelo, J.L., Mestanza, M., García, J., 2010. Heterogeneous fenton catalyst supports screening for mono azo dye degradation in contaminated wastewaters. Ind. Eng. Chem. Res. 49, 498–505. https://doi.org/10.1021/ie901212m

Rodríguez, R., Espada, J.J., Pariente, M.I., Melero, J.A., Martínez, F., Molina, R., 2016. Comparative life cycle assessment (LCA) study of heterogeneous and homogenous Fenton processes for the treatment of pharmaceutical wastewater. J. Clean. Prod. 124, 21–29. https://doi.org/10.1016/j.jclepro.2016.02.064

Rosales, E., Sanromán, M.Á., Dias-Ferreira, C., 2017. Green zero-valent iron nanoparticles synthesised using herbal extracts for degradation of dyes from wastewater. Desalin. Water Treat. 91, 159–167. https://doi.org/10.5004/dwt.2017.20713

Segura, Y., Martínez, F., Melero, J.A., 2013. Effective pharmaceutical wastewater degradation by Fenton oxidation with zero-valent iron. Appl. Catal. B Environ. 136–137, 64–69. https://doi.org/10.1016/j.apcatb.2013.01.036

Seibert, D., Borba, F.H., Bueno, F., Inticher, J.J., Módenes, A.N., Espinoza-Quiñones, F.R., Bergamasco, R., 2019. Two-stage integrated system photo-electro-Fenton and biological oxidation process assessment of sanitary landfill leachate treatment: An intermediate products study. Chem. Eng. J. 372, 471–482. https://doi.org/10.1016/j.cej.2019.04.162

Sevimli, M.F., Deliktaş, E., Şahinkaya, S., Güçlü, D., 2014. A comparative study for treatment of white liquor by different applications of Fenton process. Arab. J. Chem. 7, 1116–1123. https://doi.org/10.1016/j.arabjc.2012.12.015

Siddique, M., Farooq, R., Price, G.J., 2014. Synergistic effects of combining ultrasound with the Fenton process in the degradation of Reactive Blue 19. Ultrason. Sonochem. 21, 1206–1212. https://doi.org/10.1016/j.ultsonch.2013.12.016

Sivagami, K., Sakthivel, K.P., Nambi, I.M., 2018. Advanced oxidation processes for the treatment of tannery wastewater. J. Environ. Chem. Eng. 6, 3656–3663. https://doi.org/10.1016/j.jece.2017.06.004

Snyder, H., 2019. Literature review as a research methodology: An overview and guidelines. J. Bus. Res. 104, 333–339. https://doi.org/10.1016/j.jbusres.2019.07.039

Soon, A.N., Hameed, B.H., 2011. Heterogeneous catalytic treatment of synthetic dyes in aqueous media using Fenton and photo-assisted Fenton process. Desalination 269, 1–16. https://doi.org/10.1016/j.desal.2010.11.002

Sreeja, P.H., Sosamony, K.J., 2016. A Comparative Study of Homogeneous and Heterogeneous Photo-Fenton Process for Textile Wastewater Treatment. Procedia Technol. 24, 217–223. https://doi.org/10.1016/j.protcy.2016.05.065

Su, C.-C., Pukdee-Asa, M., Ratanatamskul, C., Lu, M.C., 2011. Effect of operating parameters on the decolorization and oxidation of textile wastewater by the fluidized-bed Fenton process. Sep. Purif. Technol. 83, 100–105. https://doi.org/10.1016/j.seppur.2011.09.021

Thomas, N., Dionysiou, D.D., Pillai, S.C., 2021. Heterogeneous Fenton catalysts : A review of recent advances. J. Hazard. Mater. 404, 124082. https://doi.org/10.1016/j.jhazmat.2020.124082

Toczyłowska-Mamińska, R., 2017. Limits and perspectives of pulp and paper industry wastewater treatment - A review. Renew. Sustain. Energy Rev. 78, 764–772. https://doi.org/10.1016/j.rser.2017.05.021

Torrades, F., García-Montaño, J., 2014. Using central composite experimental design to optimize the degradation of real dye wastewater by Fenton and photo-Fenton reactions. Dye. Pigment. 100, 184–189. https://doi.org/10.1016/j.dyepig.2013.09.004

Trapido, M., Tenno, Taavo, Goi, A., Dulova, N., Kattel, E., Klauson, D., Klein, K., Tenno, Toomas, Viisimaa, M., 2017. Bio-recalcitrant pollutants removal from wastewater with combination of the Fenton treatment and biological oxidation. J. Water Process Eng. 16, 277–282. https://doi.org/10.1016/j.jwpe.2017.02.007

Trotte, N.S.F., Aben-Athar, M.T.G., Carvalho, N.M.F., 2016. Yerba Mate Tea Extract: a Green Approach for the Synthesis of Silica Supported Iron Nanoparticles for Dye Degradation. J. Braz. Chem. Soc. 27, 2093–2104.

Umar, M., Aziz, H.A., Yusoff, M.S., 2010. Trends in the use of Fenton, electro-Fenton and photo-Fenton for the treatment of landfill leachate. Waste Manag. 30, 2113–2121. https://doi.org/10.1016/j.wasman.2010.07.003

Un, U.T., Topal, S., Oduncu, E., Ogutveren, U.B., 2015. Treatment of Tissue Paper Wastewater: Application of Electro-Fenton Method. Int. J. Environ. Sci. Dev. 6, 415–418. https://doi.org/10.7763/ijesd.2015.v6.628

Van Aken, P., Van Eyck, K., Degrève, J., Liers, S., Luyten, J., 2013. COD and AOX Removal and Biodegradability Assessment for Fenton and O3/UV Oxidation Processes: A Case Study from a Graphical Industry Wastewater. Ozone-Science Eng. 35, 16–21. https://doi.org/Doi 10.1080/01919512.2013.720552

Víctor-Ortega, M.., Ochando-Pulido, J.., Martínez-Ferez, A., 2016. Ion exchange system for the final purification of olive mill wastewater: Performance of model vs real effluent treatment. Process Saf. Environ. Prot. 103, 308–314. https://doi.org/10.1016/j.psep.2016.02.004

Vilar, V.J.P., Maldonado, M.I., Oller, I., Malato, S., Boaventura, R.A.R., 2009. Solar treatment of cork boiling and bleaching wastewaters in a pilot plant. Water Res. 43, 4050–4062. https://doi.org/10.1016/j.watres.2009.06.019

Vilardi, G., Ochando-Pulido, J.M., Stoller, M., Verdone, N., Di Palma, L., 2018. Fenton oxidation and chromium recovery from tannery wastewater by means of iron-based coated biomass as heterogeneous catalyst in fixed-bed columns. Chem. Eng. J. 351, 1–11. https://doi.org/10.1016/j.cej.2018.06.095

Vorontsov, A. V., 2019. Advancing Fenton and photo-Fenton water treatment through the catalyst design. J. Hazard. Mater. 372, 103–112. https://doi.org/10.1016/j.jhazmat.2018.04.033

Wang, C.-T., Chou, W.-L., Chung, M.-H., Kuo, Y.-M., 2010. COD removal from real dyeing wastewater by electro-Fenton technology using an activated carbon fiber cathode. Desalination 253, 129–134. https://doi.org/10.1016/j.desal.2009.11.020

Wang, C., Liu, H., Sun, Z., 2012. Heterogeneous Photo-Fenton Reaction Catalyzed by Nanosized Iron Oxides for Water Treatment. Int. J. Photoenergy 2012, 1–10. https://doi.org/10.1155/2012/801694

Wang, N., Zheng, T., Zhang, G., Wang, P., 2016. A review on Fenton-like processes for organic

wastewater treatment. J. Environ. Chem. Eng. 4, 762–787. https://doi.org/10.1016/j.jece.2015.12.016

Xie, Y., Chen, L., Liu, R., 2016. Oxidation of AOX and organic compounds in pharmaceutical wastewater in RSM-optimized-Fenton system. Chemosphere 155, 217–224. https://doi.org/10.1016/j.chemosphere.2016.04.057

Xing, Z.-P., Sun, D.-Z., 2009. Treatment of antibiotic fermentation wastewater by combined polyferric sulfate coagulation, Fenton and sedimentation process. J. Hazard. Mater. 168, 1264–1268. https://doi.org/10.1016/j.jhazmat.2009.03.008

Xu, M., Wang, Q., Hao, Y., 2007. Removal of organic carbon from wastepaper pulp effluent by lab-scale solar photo-Fenton process. J. Hazard. Mater. 148, 103–109. https://doi.org/10.1016/j.jhazmat.2007.02.015

Ye, Z., Brillas, E., Centellas, F., Cabot, P.L., Sirés, I., 2020. Expanding the application of photoelectro-Fenton treatment to urban wastewater using the Fe(III)-EDDS complex. Water Res. 169. https://doi.org/10.1016/j.watres.2019.115219

Zhang, H., Liu, J., Ou, C., Faheem, Shen, J., Yu, H., Jiao, Z., Han, W., Sun, X., Li, J., Wang, L., 2017. Reuse of Fenton sludge as an iron source for NiFe2O4 synthesis and its application in the Fenton-based process. J. Environ. Sci. (China) 53, 1–8. https://doi.org/10.1016/j.jes.2016.05.010

Zhang, H., Wu, X., Li, X., 2012. Oxidation and coagulation removal of COD from landfill leachate by Fered-Fenton process. Chem. Eng. J. 210, 188–194. https://doi.org/10.1016/j.cej.2012.08.094

Zhang, H., Xue, G., Chen, H., Li, X., 2018. Magnetic biochar catalyst derived from biological sludge and ferric sludge using hydrothermal carbonization: Preparation, characterization and its circulation in Fenton process for dyeing wastewater treatment. Chemosphere 191, 64–71. https://doi.org/10.1016/j.chemosphere.2017.10.026

Zhang, M., Dong, H., Zhao, L., Wang, D., Meng, D., 2019. A review on Fenton process for organic wastewater treatment based on optimization perspective. Sci. Total Environ. 670, 110–121. https://doi.org/10.1016/j.scitotenv.2019.03.180

Zhang, Y., Zhou, M., 2019. A critical review of the application of chelating agents to enable Fenton and Fenton-like reactions at high pH values. J. Hazard. Mater. 362, 436–450.

https://doi.org/10.1016/j.jhazmat.2018.09.035

Zhu, X., Tian, J., Liu, R., Chen, L., 2011. Optimization of Fenton and electro-Fenton oxidation of biologically treated coking wastewater using response surface methodology. Sep. Purif. Technol. 81, 444–450. https://doi.org/10.1016/j.seppur.2011.08.023